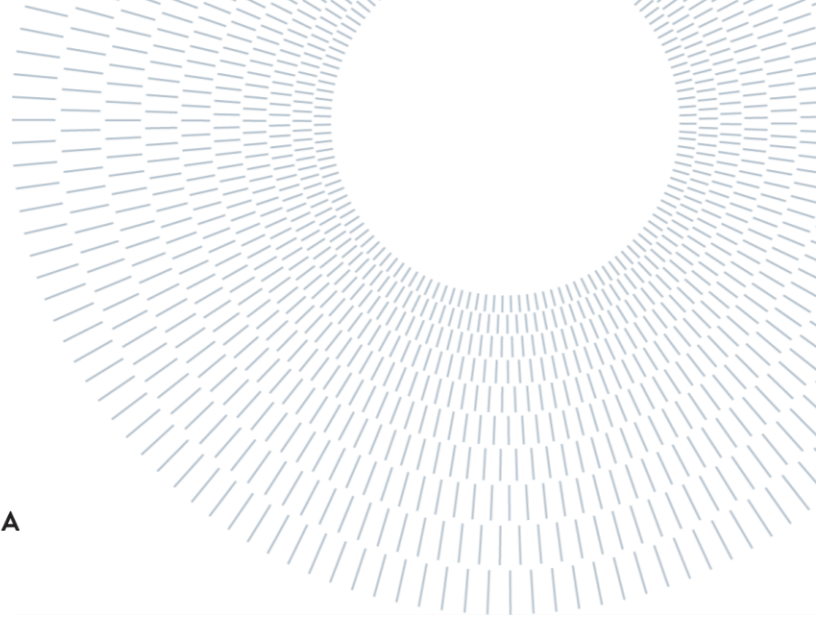




**POLITECNICO**  
MILANO 1863

DIPARTIMENTO DI ELETTRONICA  
INFORMAZIONE E BIOINGEGNERIA



# A Probabilistic Simulator for Solar-Powered Aerial Base Stations

TESI DI LAUREA MAGISTRALE IN  
Ingegneria delle Telecomunicazioni

Author: **Paniz Shahlaee**

Student ID: 940028  
Advisor: Prof. Massimo Tornatore  
Co-advisor: Philipp Wiesner  
Academic Year: 2022-23





# Acknowledgement

In this study, I benefited from joint supervision between my home university (Politecnico di Milano) and Technische Universität Berlin. I would like to thank Professor Massimo Tornatore for his support and express my sincere gratitude to Philipp Wiesner for his guidance throughout this study. Special thanks to my partner, who is always beside me despite our long-distance relationship and helps me through all the ups and downs. To my parents, without you, none of this would be possible; thank you for always encouraging me. Furthermore, I wish to show my appreciation to all my friends for their support.

At last, I would like to dedicate my thesis to all the people of my country, Iran, who got murdered by the Islamic Republic while they were demanding their freedom and human rights.

# Abstract

One of the essential visions of the next generation of communication networks is to provide reliable and global coverage. However, some events, such as disaster situations can cause damage and outage of terrestrial base stations. Therefore, Unmanned Aerial Vehicles (UAVs) have been proposed to support or even take over the terrestrial networks in such cases by offering wireless coverage as aerial base stations.

However, UAVs are powered by batteries, as opposed to terrestrial base stations, which are usually attached to the power grid. This is one of the most demanding challenges in deploying UAVs as aerial base stations since it may restrict their endurance time and communication capability. Using energy harvesting, especially solar energy, is a promising solution to address this challenge, but the amount of collected power is uncertain because of the solar irradiance variability, which makes it difficult for the practitioners to manage and equip the solar-powered UAV to establish a network in the desired area. Therefore, solar power forecasts can be used to predict the amount of harvested energy by the UAV to plan its mission.

On the other hand, testing the actual equipment can be unfeasible from an economic and risk point of view. Therefore, simulation plays a vital role in such cases. Researchers developed different simulators for UAVs based on the different use of these aerial vehicles, but there is no simulator that provides the prediction of the behavior of solar-powered UAVs using the solar irradiance forecast from a power consumption point of view to empower practitioners in making better informed decisions about how to equip their UAVs depending on the mission and network requirements.

This study aims to provide an analytical tool to simulate the behavior of the solar-powered UAV by modeling its energy consumption and providing information for operators by using probabilistic solar irradiance forecasting. The tool uses the inputs based on the details of the mission and, by simulating it, will provide information such as the duration that the UAV may be active in the mission, the status of the UAV, and also the battery charge level at the end of the simulation. Moreover, it provides a log file that consists of the detailed actions of the UAV during the simulation.

Based on the emergency scenario implemented through the provided tool, we demonstrate its usefulness and capabilities. Our experimental evaluation shows a

maximum 5% difference between the predicted outcomes and the actual outcomes of the simulation. The runtime of the simulation for the scenario in different experiments was, on average, around one minute, confirming its applicability for pre-deployment evaluation. Moreover, the experiments show the impact of different aspects, such as the start time of the mission, the battery threshold for returning to the initial station and distance to the destination of the scenario on the outputs.

In conclusion, our tool can provide informative details to the operators, and its good performance and short execution time help them to make the best decision on equipping the UAV and assess the risk with a high amount of certainty in a short amount of time.

**Key-words:** Unmanned aerial vehicles (UAVs), Aerial base stations, Solar-powered UAVs, Energy harvesting, Probabilistic forecasting, Simulation

## Abstract in lingua italiana

Una delle visioni essenziali della prossima generazione di reti di comunicazione è quella di fornire una copertura affidabile e globale. Tuttavia, alcuni eventi, come le situazioni di emergenza, possono causare danni e interruzioni delle stazioni base terrestri. Pertanto, i veicoli aerei senza equipaggio (UAV) sono stati proposti per supportare o addirittura assumere il controllo delle reti terrestri in tali casi offrendo copertura wireless come stazioni base aeree.

Tuttavia, gli UAV sono alimentati da batterie, al contrario delle stazioni base terrestri, che di solito sono collegate alla rete elettrica. Questa è una delle sfide più impegnative nel dispiegamento di UAV come stazioni base aeree poiché potrebbe limitare il tempo di resistenza e la capacità di comunicazione. L'utilizzo della raccolta di energia, in particolare l'energia solare, è una soluzione promettente per affrontare questa sfida, ma la quantità di energia raccolta è incerta a causa della variabilità dell'irraggiamento solare, che rende difficile per i professionisti gestire ed equipaggiare l'UAV a energia solare per stabilire una rete nell'area desiderata. Pertanto, le previsioni sull'energia solare possono essere utilizzate per prevedere la quantità di energia raccolta dall'UAV per pianificare la sua missione.

D'altra parte, testare l'attrezzatura reale può essere irrealizzabile da un punto di vista economico e di rischio. Pertanto, la simulazione gioca un ruolo fondamentale in tali casi. I ricercatori hanno sviluppato diversi simulatori per UAV basati sul diverso utilizzo di questi veicoli aerei, ma non esiste un simulatore che fornisca la previsione del comportamento degli UAV a energia solare utilizzando la previsione dell'irraggiamento solare dal punto di vista del consumo di energia per consentire ai professionisti di fare decisioni più informate su come equipaggiare i loro UAV a seconda della missione e dei requisiti di rete.

Questo studio mira a fornire uno strumento analitico per simulare il comportamento dell'UAV a energia solare modellando il suo consumo energetico e fornendo informazioni agli operatori utilizzando la previsione probabilistica dell'irraggiamento solare. Lo strumento utilizza gli input in base ai dettagli della missione e, simulandola, fornirà informazioni come la durata che l'UAV può essere attivo nella missione, lo stato dell'UAV e anche il livello di carica della batteria alla fine della simulazione. Inoltre, fornisce un file di registro che consiste nelle azioni dettagliate dell'UAV durante la simulazione.

Sulla base dello scenario di emergenza implementato attraverso lo strumento fornito, ne dimostriamo l'utilità e le capacità. La nostra valutazione sperimentale mostra una differenza massima del 5% tra i risultati previsti e i risultati effettivi della simulazione. Il tempo di esecuzione della simulazione per lo scenario in diversi esperimenti è stato, in media, di circa un minuto, a conferma della sua applicabilità per la valutazione pre-distribuzione. Inoltre, gli esperimenti mostrano l'impatto di diversi aspetti, come l'ora di inizio della missione, la soglia della batteria per il ritorno alla stazione iniziale e la distanza alla destinazione dello scenario sulle uscite.

In conclusione, il nostro strumento può fornire dettagli informativi agli operatori e le sue buone prestazioni e il breve tempo di esecuzione li aiutano a prendere la decisione migliore sull'equipaggiamento dell'UAV e a valutare il rischio con un'elevata certezza in un breve lasso di tempo.

**Key-words:** Unmanned aerial vehicles (UAVs), Aerial base stations, Solar-powered UAVs, Energy harvesting, Probabilistic forecasting, Simulation

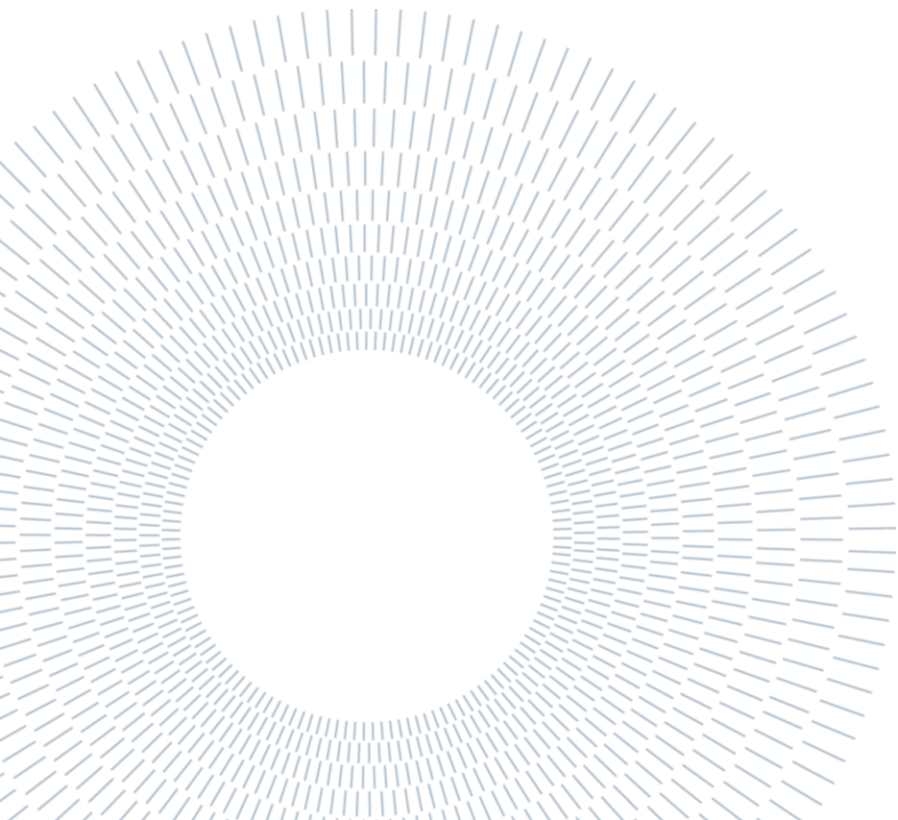


# Table of Contents

|   |     |
|---|-----|
| Acknowledgement.....  | i   |
| Abstract.....   | ii  |
| Abstract in lingua italiana.....                                | iv  |
| Table of Contents .....   | vii |
| 1 Introduction.....   | 1   |
| 1.1 Outline of the Thesis .....                                 | 3   |
| 2 Background.....   | 5   |
| 2.1 UAV Definition and History .....                            | 5   |
| 2.2 UAV Flying Mechanism.....                                   | 6   |
| 2.3 UAV in Beyond 5G and 6G.....                                | 7   |
| 2.3.1 MIMO .....  | 7   |
| 2.3.2 Beamforming .....   | 8   |
| 2.3.3 mmWave .....  | 9   |
| 2.3.4 MIMO, beamforming, and mmWave in UAV Communications ..... | 9   |
| 2.3.5 Multiple Access and Backhaul .....                        | 10  |
| 2.4 Power and energy consumption .....                          | 12  |
| 2.5 Energy Harvesting .....                                     | 12  |
| 2.6 Probabilistic Weather Forecasting .....                     | 14  |
| 2.7 Discrete Event Simulator.....                               | 14  |
| 3 Related Works.....  | 15  |

|       |  |    |
|-------|--|----|
| 3.1   | UAV Simulators.....  | 15 |
| 3.2   | Addressing Limited Onboard Battery of UAVs as Aerial Base Stations ..... | 16 |
| 3.3   | Solar-Powered UAVs.....  | 18 |
| 4     | Approach to Implementing the Simulator.....                              | 19 |
| 4.1   | Discrete-Event Simulation Components.....                                | 20 |
| 4.1.1 | Mission Monitor and Control Process .....                                | 20 |
| 4.1.2 | UAV State Process.....   | 21 |
| 4.1.3 | Battery Process .....  | 21 |
| 4.1.4 | Interaction Between Processes .....                                      | 21 |
| 4.2   | UAV Energy Model.....  | 24 |
| 4.2.1 | Flying Energy Consumption Model.....                                     | 24 |
| 4.2.2 | Communication Energy Consumption Model .....                             | 27 |
| 4.3   | Battery Charging/Discharging Model .....                                 | 28 |
| 4.4   | Solar Cell Harvesting Energy .....                                       | 29 |
| 4.5   | Probabilistic Solar Irradiance Forecasting .....                         | 31 |
| 4.6   | Tool Components .....  | 31 |
| 4.6.1 | Input.....   | 32 |
| 4.6.2 | Simulation Process.....  | 33 |
| 4.6.3 | Output.....  | 34 |
| 5     | Evaluation.....  | 36 |
| 5.1   | Scenario setup .....   | 36 |
| 5.1.1 | Emergency Scenario.....  | 36 |
| 5.1.2 | Implementation of the Simulator.....                                     | 37 |
| 5.1.3 | Solcast Probabilistic Forecasting.....                                   | 38 |
| 5.2   | Experiment .....   | 39 |
| 5.2.1 | With and Without Energy Harvesting.....                                  | 40 |

|       |  |    |
|-------|--|----|
| 5.2.2 | Different Start Times with Two Different Initial Battery Level ..... | 41 |
| 5.2.3 | Predicted Outputs vs. Actual Outputs .....                           | 44 |
| 5.2.4 | Using Different Equipment .....                                      | 47 |
| 6     | Conclusion and Future Work.....                                      | 51 |
|       | List of Figures .....  | 53 |
|       | List of Tables.....  | 55 |
|       | Bibliography .....   | 56 |

# 1 Introduction

Unmanned aerial vehicles (UAVs) are aircraft with no human pilot and are mostly controlled and managed remotely or by embedded autonomous computer programs. The unique capabilities of UAVs, also known as drones, relating to their high mobility, flexibility of deployment, and remote operation make them a solution for a wide range of applications such as civil, commercial, and military services. The global UAV market was valued at US\$ 20.68 billion in 2017 and is expected to reach US\$ 59.82 billion by 2026 [1]. UAV-enabled wireless communications have attracted the attention of both academics and industry in recent years due to their cost-effectivity, on-demand operation, characteristics of line of sight (LoS) communication links, large coverage, ease of deployment and low cost in comparison to terrestrial communication systems [2] [3].

Despite improvements of 5G over 4G in terms of data rate, spectrum efficiency, traffic capacity, and latency, 5G still faces many challenges to satisfy all the requirements of future networks and applications and will not be able to meet all the future requirements in 2030 [4]. One of the visions of 6G (beyond 5G) networks is to provide global coverage. As a result, the sixth generation of cellular networks is expected to support remote and high-mobility communications, as well as space-air-ground-sea all-coverage communications, computing, sensing, and full spectral integration [5]. In literature, UAVs are one of the important technologies mentioned to fulfill the demand for global coverage in the next generation of communication networks to provide non-terrestrial networks to achieve a space-air-ground-sea integrated communication network [4]. On the other hand, in an emergency situation, when the terrestrial cellular network is down, it is essential to have communication infrastructure that can be used on-demand so that communication can be quickly restored. In this regard, UAVs can be used to establish aerial base stations (ABSs) and provide wireless coverage, especially in emergency areas, by acting as aerial wireless base stations. Therefore, wireless communication links can be established quickly using UAVs. In this way, UAVs became a point of interest for researchers in the field of 6G (beyond 5G) [5] [4]. Overall, UAVs can be used in 5G networks, but they will play a vital role in fulfilling the full coverage characteristic of the 6G networks vision.

Unlike terrestrial base stations (BSs), which are almost always connected to the power grid, UAVs are powered by batteries. This is one of the biggest challenges in the case of using UAVs as ABSs, which may limit their endurance duration and communication performance [4] [6].

To address the problem of limited onboard energy and increase the active time in UAVs, we can refer to harvesting power from renewable sources (e.g., solar power, which we used in this study), which can be low-cost and environmentally-friendly alternatives. A solar-powered UAV recharges its battery using solar power gathered from daylight. In some circumstances and depending on the conditions of the environment, the power that has been stored may even be sufficient to allow the UAV to remain continuously active all through the night and possibly even subsequent day-night cycles [7], so the endurance time increases significantly. In this case, solar-powered UAVs (equipped with solar panels) can be great candidates when UAVs need to be active for an extended amount of time, like when they are used as the aerial base station in emergency situations when BSs are down. However, the amount of harvested power is random due to the uncertainty and variability of solar power [6]. Moreover, managing and planning the mission of the UAVs is important, especially in the case of emergency. In this regard, the practitioners need to have information about how their solar-powered UAVs may act at different times of day and with various equipment and they need to know how to equip the UAV to provide service for a maximum amount of time or how long their UAVs will be running with a certain equipment installation. The equipment can be considered as the different available onboard batteries with a certain amount of energy level, solar panels with different amounts of area, and the characteristics of the communication network that the UAV can provide. Thus, forecasting solar irradiance becomes essential to learn how long the UAV will be operational during its mission. Moreover, in most cases, using the real prototype and systems is not feasible because of the cost and risks. Therefore, simulation plays a vital role in the mention use case of UAVs.

The total power consumption of the UAVs as ABSs consists of the power needed for mechanical parts tasked with flying and the power required for communicating with the users. Considering the technologies and equipment of solar-powered UAVs, we can refer to the factors that impact the energy consumption and energy harvesting of solar-powered UAVs. Therefore, any change in effecting parameters in flying and communicating power consumption of the UAV has an impact on the total power consumption. The important influential factors on flying energy consumption are: 1) flying distance, 2) vertical and horizontal velocity and 3) total weight of the UAV. Also, it is essential that the UAVs be equipped with proper mobile communication capabilities. Thus, UAVs can be used as aerial base stations in combination with mmWave and massive MIMO, which has a large available bandwidth and can provide multi-Gbps data rates [8] but here, also any change in communication characteristics such as the number

of antennas and number of radio frequency chains to providing the network will change the power consumption of communication. Another important characteristic of the UAV that is considered is its flying mechanism. Due to the need to hover on the top of the service area and the capability of flying vertically, rotary-wing UAVs are a good candidate to use in 6G networks. Additionally, when a UAV flies towards an area to provide the service, it is important to have a battery threshold to know when it is time to fly back to the UAV's base station and this threshold should be decided in order not to have a negative impact in the operation; if it is too high, it can prevent the UAV from reaching the destination or if it is too low, it can crash the UAV. Also, the area of solar panel and battery characteristics has an impact on the amount of harvested power, and their weight also affects the power consumption.

Based on what is mentioned above, there are many factors that have an impact on the total energy needed by the UAVs to act as the aerial base station and provide service in a specific area, and using solar power to address the limited onboard energy makes the management and planning the mission of a UAV complicated based on the affecting factors and variability of energy source (solar energy).

The aim of this thesis is to develop a tool for aiding the operators to know how long a single solar-powered UAV will be operating and how long the maximum endurance time of them by using the simulation of the power consumption model of the UAV and using solar power forecasting to estimate the active time of UAV during different states of its mission. In this way, the operators would know how to equip the UAVs with different technologies and solar panels in order to fulfill the need of the UAV in different situations to provide wireless communication. Therefore, our tool provides information about the different states of UAV at a given time and helps the operators to make the best decision for their solar-powered UAV ABSs.

## 1.1 Outline of the Thesis

The structure for this thesis is explained in the following:

Chapter 2 gives background information on the topics of this study. First, we see the definition and history of the UAV and its importance during the time. Second, the flying mechanism of the UAVs as an important factor for choosing them is presented. Third, there is a section to undertake testing the technologies that are used to align the UAVs for providing wireless communications in 5G and 6G networks. Fourth, we briefly explain the concept of energy and power consumption in UAV. Energy harvesting is explained in the fifth part. Definition of probabilistic weather forecasting and discrete event simulator are discussed in sixth and seventh sections, respectively.

Chapter 3 reviews related works to address the current problem and describes the gaps in those efforts and novelty of our study. First different existing simulators for UAVs are presented. In second section, different approaches for addressing the limited onboard energy for the UAVs are explained. And in the last part, existing studies on solar-powered UAVs are presented.

Chapter 4 presents the methodology and approach for implementing our simulation tool. First, the components of the discrete event simulator are explained and in the second part the energy consumption models of the UAV in different actions are defined. Third section is dedicated to the type and charging/discharging model of the battery that it is simulated the battery of the UAV. In the fourth and fifth parts, solar energy harvesting and probabilistic solar irradiance forecasting are explained, respectively. The sixth part contains the description of the components of the tool as inputs, process, and outputs.

Chapter 5 will cover a scenario in which we have determined to evaluate the potential of the tool. The implementation of the scenario using the simulator and using the probabilistic solar irradiance are explained in the first section, and then in the second section, there are some experiments to evaluate the performance of the tool in practice.

Chapter 6 concludes our work and possible directions for further research are suggested.

## 2 Background

An overview of fundamental concepts and terms in the UAV communication sector which are used in this study is given in this chapter. In the first Section 2.1, a brief history and definition of UAVs are given to understand the importance of these vehicles in time. Section 2.2 explains the flying mechanisms for UAVs because it is one of the most important factors that should be considered for using the right UAV for different uses. The terms and importance of UAVs in recent and future wireless communications are studied in Section 2.3. Section 2.4 explains the power and energy related units, and Section 2.5 concludes with the term energy harvesting. Section 2.6 explains the fundamental aspects of probabilistic weather forecasting, and Section 2.7 covers an explanation of the discrete event simulator.

### 2.1 UAV Definition and History

Unmanned Aerial Vehicles, more commonly referred to as UAVs, are aircraft that have the ability to fly and stay airborne without the need for a human pilot, which enables them to fly either autonomously or under remote control. UAVs, also known as drones, basically comprises a battery, computing unit, sensors, and actuators, and they can be modified based on their application. Due to not needing an onboard pilot and being able to be controlled remotely, the primary use of UAVs was for military purposes in the hostile area for remote surveillance and armed attack to minimize pilot losses [9]. Nowadays, UAVs attract attention in numerous applications in civil and commercial such as aerial inspection, photography, precision agriculture, traffic control, search and rescue, package delivery, and telecommunications. UAVs can be outfitted with different technologies and equipment to fulfill their application demands. The potential size of the UAV sector is significant, with estimates of reaching US\$ 59.82 billion by 2026 [1] in the global market and the creation of tens of thousands of new employment over the next decade. Therefore, UAVs have emerged as a promising technology that will provide many economic prospects alongside its applications in the coming decade.

## 2.2 UAV Flying Mechanism

It is important to use the appropriate UAV technology to satisfy the requirements of the application and objectives of the mission, as there are several technological choices that should be considered for using UAVs for specific applications. The application of the UAVs in this study is related to their mission to provide a network as an aerial base station (ABS). One of the factors that should be considered is the flying mechanism of the UAVs. They can be categorized as fixed-wing and rotary-wing UAVs. Fixed-wing drones glide over the air, which gives them a considerable advantage in terms of energy efficiency and also allows them to carry a heavy payload. The gliding also allows fixed-wing UAVs to fly faster. Rotary-wing drones (also known as Multi-rotor drones) are able to take off and land vertically and can hover over a fixed location which makes them suitable for establishing the communication link in the desired location by hovering. However, rotary-wing UAVs consume significant power as they have to fight against gravity constantly. On the other hand, vertical landing and take off is not possible for fixed-wing UAVs, and they need a runway for take-off and landing; they also are not able to hover over a fixed location and are more expensive than multi-rotor drones [10].

Propulsion power consumption of fixed and rotary wing UAVs are modeled in [2] and [11] respectively. As it is shown in Figure 2-1 [12], for both kinds of mechanisms, the required power first decreases and then increases, so we can say that flying at low and high speeds is not power efficient in both cases. Regarding differences, the capability of keeping the UAV stationary at fix position and the ability to vertically take off and landing would be more necessary in situations where the UAV wants to hover above the service area and provide the network to the ground users. Moreover, the ability to take off and land vertically in the rotary-wing UAVs makes them more popular in the use cases of UAV communication [13].

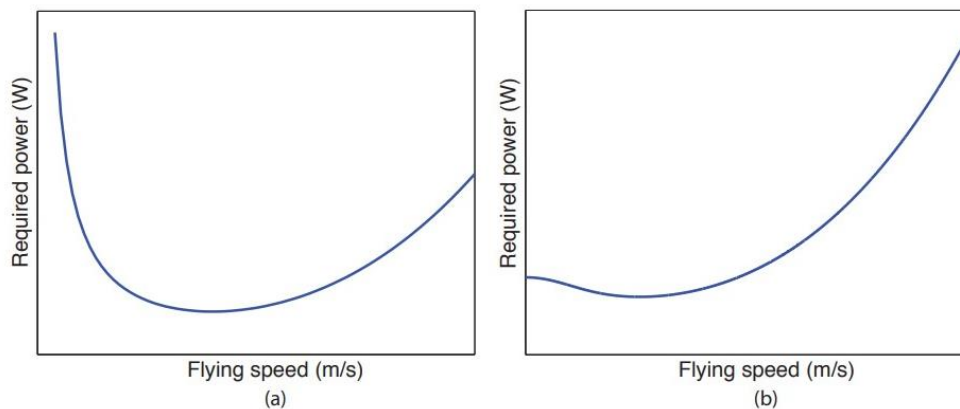


Figure 2-1: Adopted from [5], Figure5. propulsion power consumption vs. UAV flying speed: a) Fixed-wing UAVs b) Rotary-wing UAVs

## 2.3 UAV in Beyond 5G and 6G

Over the past few years, there has been considerable progress in wireless communication technologies. The fifth generation (5G) wireless networks made significantly advanced technologies beyond 4G, such as new frequency bands like millimeter-wave (mmWave) spectrum, massive multiple-input multiple-output (MIMO), and ultra-dense network (UDN). In such a way, there is an improvement in data rate, spectrum efficiency, traffic capacity, and latency compared with 4G. Nonetheless, 5G still faces some challenges and will not be able to satisfy all the requirements in 2030+ [4]. Some required demands beyond 5G wireless networks (6G) are to provide more capacity, lower latency, and higher data transmission. More importantly, the 6G network is expected to support remote and high mobility communications, as well as space-air-ground-sea all-coverage communications, and provide full wireless coverage [5]. To achieve global coverage, a space-air-ground-sea integrated network utilizes satellite communication, UAV communication, terrestrial communication, and marine communication. UAVs have been seen as a vital component and a potential technology in future wireless networks due to intrinsic properties such as flexibility, mobility, and adjustable altitude, and they can be used as aerial communication platforms [4].

Communication networks based on unmanned aerial vehicles include numerous distinctive properties, such as different and flexible topologies, on-demand relocation, extra-degree of freedom due to 3D transmission characteristics, and improved coverage due to higher line-of-sight (LoS) connections with ground users. As mentioned above, UAVs can be used for ubiquitous coverage. They can act as an aerial base station as a supplement or a replacement for an existing terrestrial base station when the ground base station is damaged or out of service [14].

### 2.3.1 MIMO

One of the demands of 5G was the application of massive multiple input multiple output (MIMO) antennas which use a large number of antennas at the base station (BS). MIMO is one of the most widely used methods to increase spectrum efficiency. The information rate that can be sent across a particular bandwidth in communication networks is referred to as spectrum efficiency (in bits per second per Hz). It represents how efficiently the physical layer protocol uses a specific spectrum [15]. Moreover, multi-antenna arrays and spatial multiplexing are used in massive MIMO to transmit independent and individually encoded data signals, which are referred to as "streams." These allow simultaneous communications with multiple user equipment (UE).

### 2.3.2 Beamforming

Beamforming is a technique in which the radio signals radiate in a particular direction, generally in the direction of a certain receiving device.

Three different methods are used for implementing the beamforming:

Analog beamforming (ABF): is the basic approach in which the signal phase is shifted in the analog domain. It uses simple electronic components and uses only one radio frequency (RF) chain, which theoretically makes it an ideal choice for achieving low power consumption. Therefore, it is a cost-effective approach to implement beamforming. However, since it works with one RF chain, it generates one single beam and one data stream at a time which limits the effectiveness in communication networks (5G and 6G) where multiple beams are required [16].

Digital beamforming: in this approach, each antenna has its own RF chain, and the signals are separately pre-coded digitally with amplitude and phase modification by baseband processing. In this way, digital beamforming enables the flexibility of a single antenna array to serve multiple beams (multiple users). This flexibility is an ideal option to fulfill the requirement of multiple beams in communication networks, but its high power consumption places a limitation on using this approach.

Hybrid beamforming (HBF): this approach uses the advantages of previous ones and settles a simple transceiver design by combining RF analog beamformers with low-dimensional baseband digital beamformers. In such a way, hybrid beamforming provides a balance between digital beamforming's flexibility and the lower power consumption and cost-effectivity of analog beamforming [16]. As it can be seen in Figure 2-2, the base band processing is done in digital domain while the antenna elements are still driven from analog phaseshifters.

From the consuming power point of view, the authors in [16] showed that HBF always consumes less power compared to ABF.

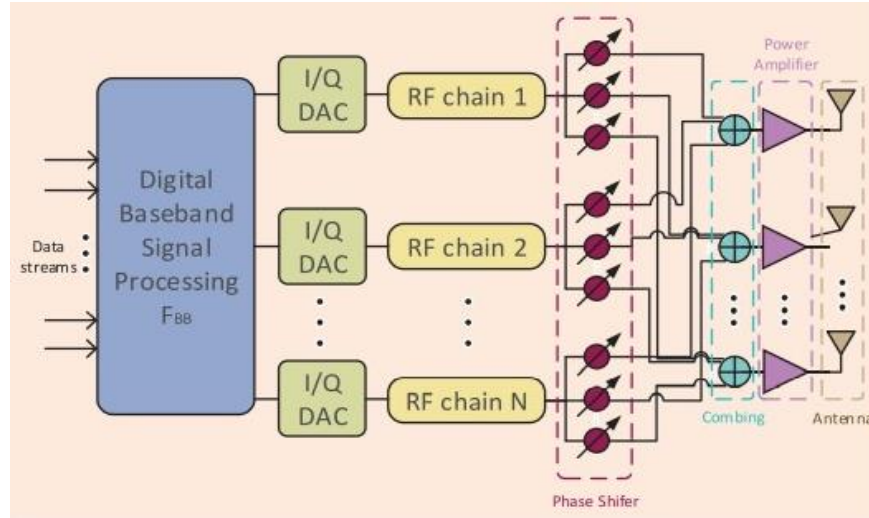


Figure 2-2: Adopted from [16], Figure3. HBF architecture with multiple RF chains

### 2.3.3 mmWave

Millimeter waves (mmWave) have a corresponding wavelength between 1mm to 10mm and occupy the highest RF frequency spectrum (30GHz-300GHz), namely Extremely High Frequency (EHF). mmWaves are the highest frequencies that can be used to transmit data in wireless communications, and the higher frequencies provide the potential for greater capacity. More available spectrum (bandwidth) in mmWave allows for wider channels which leads to maximizing the capacity and less interference.

Wideband transmission in the mmWave frequency ranges is generally regarded as a significant component of 5G new radio (NR) and will play an even more prominent role in 6G [17]. mmWave signals, on the other hand, suffer from significant propagation loss, which includes free-space path loss, atmospheric and molecular absorption, and rain attenuation. Thus, in mmWave communication systems, directional antennas or antenna arrays should be used to provide high beam gains and extend transmission range, where beamforming plays a vital role [17]. Furthermore, beamforming has the ability to enhance spectrum efficiency via coherent combining and higher antenna aperture [18].

### 2.3.4 MIMO, beamforming, and mmWave in UAV Communications

UAV communications often require high data rate connections. Due to severe spectrum scarcity and interference in the sub-6 GHz band, the microwave band, which has been widely used in terrestrial communication networks, may be unable to support UAV communications. However, mmWave communication has a large amount of available spectrum, which can provide high-rate transmission. Using the UAVs equipped with

massive multiple input multiple output (MIMO) beamforming is an alternative for improving the propagation performance of mm-wave systems and achieving the objectives of future 6G wireless networks. On the one hand, UAVs have the ability to fly out of blockage zones in order to establish line-of-sight (LoS) connections. On the other hand, as mentioned before, the wavelength ( $\lambda$ ) of mmWaves is between 1 to 10mm. In this case, the distance between every two antennas will be between 0.5mm to 5mm ( $\lambda/2$ ). Therefore, it is possible to fit a large number of antennas into a small UAV. Moreover, the small distance between antennas makes the beam narrower and more concentrate. This allows the beamforming to be properly built, which is necessary in order to overcome the limitations of mm-wave communications, provide the array gain and reduce the co-channel interference [19] [15].

Millimeter-wave (mmWave) technology offers huge available bandwidth and multi-Gbps data rates. The short wavelength of mmWave signals allows multiple antenna elements to be placed into a small UAV. Moreover, massive MIMO can provide a very powerful beamforming system for the high number of antennas [19].

### 2.3.5 Multiple Access and Backhaul

For UAVs to help ground users and connect to the core network, they need to have both multiple access and backhaul.

NOMA (Non-Orthogonal Multiple Access) is a new technology that will help wireless communication networks support large numbers of users [20]. The transmitter transmits different signals while differentiating them with varying power levels inside the same orthogonal resource block. At the receiver, the signals are decoded one at a time with the help of a technology called successive interference cancellation (SIC). NOMA is particularly spectrum efficient because it multiplexes users in power domains and transmits their data at the same frequency and at the same time. As it can be seen in Figure 2-3, there are two users (UE-1 and UE-2) which are at the different distance from the base station. By using NOMA, more power is allocated to the UE-2 which is in a further location, so the UE-2 can decode its signal by considering the UE-1 signal as noise and UE-1 recover its signal by using the SIC. In such a way, using this technology among the mmWave and MIMO, helps us to provide the network to more users at the same time.

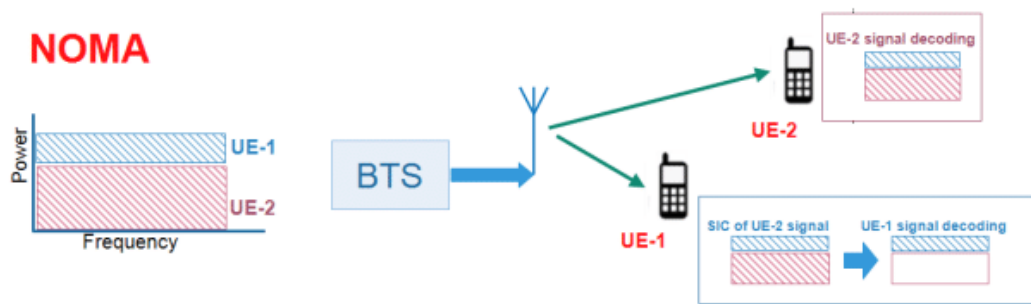


Figure 2-3: From [60], downlink NOMA

Unlike terrestrial BSs, UAVs cannot establish wired backhaul connections via optical fibers. Consequently, wireless backhaul is required for them. Based on the characteristics of the mmWave, which are mentioned in (2.3.3), it can be a proper technology to use also for the backhaul communication for the UAVs. Due to the need for wireless transmission for the backhaul connection, IAB (Integrated Access and Backhaul), also known as self-backhauling, is a crucial subject for mmWave-UAV aerial base stations in order to enhance the network's adaptability. To be more specific (see Figure 2-4), a UAV may perform backhaul through the access connection of a terrestrial macro-BS or another UAV aerial base station. After that, the UAV may join the backbone network through either a direct connection (single hop) or via a series of intermediate nodes (multiple hops). It is important to remember that IAB is free to use any available frequency band in the access link. By using IAB, the UAV planar antenna can be used for both communicating and backhauling [21].

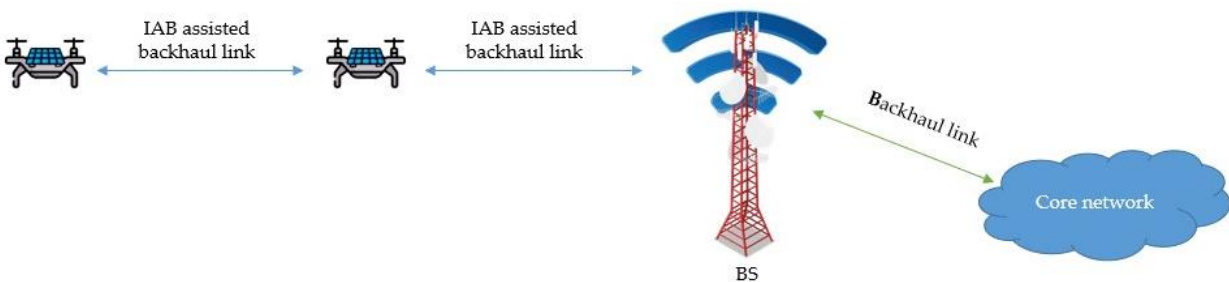


Figure 2-4: Potential IAB network for UAV aerial base stations

## 2.4 Power and energy consumption

"Energy usage" and "energy consumption" refer to electrical energy conversion. Every electrical circuit has an energy source and a consumer. An electric charge in the energy source creates a voltage that causes electric currents to flow through the consumer part. Power is the rate at which energy is transformed. Watt [W] is the SI unit of power (including electrical power). By knowing the voltage of the circuit as well as the amount of current the device receives, it is possible to compute the power of an electric device. In other words, one Watt [W] electrical power [P] is defined by one ampere [A] current flow [I] at one volt [v] electrical potential difference (V).

$$P[W] = I[A] * V[v] \quad (2-1)$$

On the other hand, electrical power defines the rate at which work is performed by consuming energy. Moreover, energy (E) refers to the capacity to perform work, and Joule (J) is the commonly used SI unit for it, so one Watt can be expressed as Joule per second as in Equation(2-2).

$$P[W] = E[J]/T[s] \quad (2-2)$$

Considering the above Equation(2-2), we can see that another unit for energy would be Watt-second(*Ws*) which represents the needed energy to consume or produce electrical power during time. The unit that usually is used for energy in reports and bills is watt-hour (*Wh*). Therefore,  $1Wh = 3600 Ws = 3600 J$ .

## 2.5 Energy Harvesting

The term "energy harvesting" refers to the process of collecting and converting easily accessible energy from the surrounding environment into useful electrical energy. The electrical energy is prepared for either immediate use or for accumulation and storage for later use. This provides an alternative way to get power in locations where there is no access to the power grid to recharge the batteries. Since the amount of energy stored in batteries is limited, they must be periodically replaced or recharged. Using energy harvesting with the appropriate application will decrease the need for physical interventions for charging, and devices will be developed to be used wireless. In such a way, the devices equipped with energy harvesting can be used in environments that are hard to access. Therefore, energy harvesting is a technique that can be used to replace or, at the very least, improve the usage of batteries and devices.

Energy harvesting can be categorized based on the form of energy that is used for energy scavenging. For example, solar harvesting devices scavenge and convert solar energy from the sun into usable electrical energy [22]. Usually, the energy sources that can be harvested are heat energy, light energy (sunlight or artificial light), kinetic energy (vibration or mechanical stress), and RF energy.

Energy harvesting systems typically include three primary parts Figure 2-5, a transducer that is particular to the application, an interface circuit, and a storage unit. The transducer, which is also called the energy harvesting unit, converts the collected energy (from the environment) to electrical energy. The transducers used for heat, light, kinetic, and RF energy, respectively, are thermoelectric, photovoltaic (PV), piezoelectric, and RF. The responsibility of the interface circuit unit, which is also known as power management, is to make the energy level work perfectly with the receiver or load by performing different approaches like voltage regulation or rectification. And also another function of the interface unit is to get the most energy out of the harvesting unit. Having a storage unit can prevent problems when the harvesting intervals are long, or the energy source is not available in real-time and helps to avoid running out of energy.

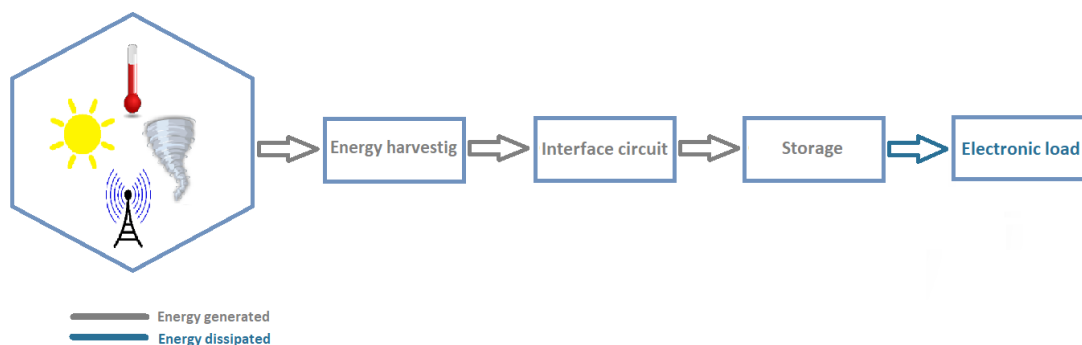


Figure 2-5: Basic components of an energy harvesting system

In [23], it is indicated that, in comparison between different types of harvesting sources, solar energy may provide more power. Moreover, the availability and nonpolluting potentials of solar energy and its ability to collect solar energy without any need for specific circumstances like motions (vibrations), the presence of electromagnetic fields, or temperature changes make it one of the most common sources of energy harvesting.

As mentioned before, the suitable transducer for solar energy harvesting is photovoltaic. To convert sunlight into electrical power, solar cells are used in these systems. Photons of light excite electrons into a higher level of energy and perform as charge carriers to produce an electric current [23].

## 2.6 Probabilistic Weather Forecasting

One of the most significant issues in forecasting solar variability is that deterministic forecasts (those that give only one number) do not offer end users an adequate level of decision-making information. Not all forecasts have the same chance of being correct, and variable weather and climatic circumstances have a direct impact on forecast likelihood. Therefore, forecasting of weather quantities and events has shifted to probabilistic forecasts that are expressed as probability distributions. A probabilistic forecast quantifies the degree of uncertainty in a prediction and allows optimal decisions to be made [24].

## 2.7 Discrete Event Simulator

Simulation is a way to study a model of an actual system by using a mathematical model. The method for simulating a dynamic system is a method known as discrete event simulation (DES). Using discrete event simulation, the actual world is represented mathematically, its dynamics are simulated on an event-by-event basis, and detailed performance reports are produced [25]. Moreover, DES is used to simulate real-world systems that may be divided into a number of logically distinct processes that progress independently across time. Each event takes place on a particular process and is given a logical time (a timestamp). One or more additional processes may be output from each event. The outcome's content could result in the generation of new events that will be handled at a specific future logical time. Queuing theory acts as the theoretical foundation for the statistical paradigm that underpins DES. Tracking the changing state conditions of a process over time is an essential part of discrete event simulation. This type of simulation works exceptionally well for modeling input details and determining detailed system outputs.

## 3 Related Works

This chapter reviews relevant work in order to highlight the contributions of earlier research and explain the contributions of this thesis. In particular, it is intended to show that none of the previous studies is able to meet the requirements mentioned in Section 1. Section 3.1 overviews the different UAV simulators based on their purposes. Section 3.2 highlights the studies and approaches for addressing the limited onboard batteries for the UAVs and Section 3.3 consists of the previous researches on the solar-powered UAVs.

### 3.1 UAV Simulators

Simulators are vital since most tests using actual devices or systems are impractical because of the expense and risk associated. There are some UAV simulators that enable a variety of sensors, such as cameras, lidars, GPS, microphones, gas sensors, and so on. There is no single simulator that can be used for all purposes. The appropriate simulator is chosen based on both the purposes and the many features provided by the simulator. Some of these simulators, like XPlane [26], Flightgear [27], and JMavSim [28], are designed to simulate UAV physics for training pilots. Other simulators for UAVs are Microsoft Airsim [29] and UE4Sim [30], which also show UAVs' motion planning compared to the above simulators. The authors in [31] suggested a software simulator in the agricultural area capable of defining particular variables and parameters as well as testing UAV team control and coordination procedures. To deal with parasites, these papers propose innovative strategies for UAV coordination and surveillance of a specified location. The suggested methodologies demonstrate how UAV behavior and performance alter when multiple restrictions, such as communication coverage range, and drone resources, are considered. In another study [32] they proposed Aerial Vehicle Network Simulator, a hybrid software-based simulator (AVENS). This simulator combines X-Plane and OMNeT++ with LARISSA (A layered architecture model for system connectivity in UAS). They combined a number of networking protocols. The two simulators have distinct features: X-Plane offers flight control, whereas OMNeT++

measures network metrics like throughput, packet loss, and so on. XML files are used to communicate information between the two environments. All mentioned simulators of UAVs are focused on the flying and motion, and networking of the UAVs, and they have not addressed the battery and energy consumption of the UAVs.

In another work [33], the authors proposed a discrete simulation framework for mobile robotic systems with an emphasis on energy conservation and node replacement procedures using several UAVs. The simulation framework's objective is to assess and then improve management procedures, and the limited onboard energy has been addressed by the replacement of UAV. However, the communication process has been represented with simple implementation, which does not meet the requirements of wireless communication.

## 3.2 Addressing Limited Onboard Battery of UAVs as Aerial Base Stations

UAVs have attracted a lot of interest in recent years for both military and commercial uses. Due to their low cost and flexible deployment, unmanned aerial vehicles (UAVs) are expected to play important roles in Sixth Generation (6G) networks. The 6G network is planned to be an all-coverage network that will allow connections everywhere, including in the air, ground, and underwater. UAVs have the capability to provide airborne wireless coverage in a flexible manner. They can operate as aerial base stations for ground users as relays to connect ground users [4]. For instance, when there is no terrestrial communication infrastructure or the ground base station is damaged, and out of service, UAVs can be used as aerial base stations to provide network coverage temporarily.

In comparison to current ground-based stations, UAV aerial base stations may offer much improved performance in terms of coverage, load balancing, spectrum efficiency, and user experience since they can be quickly deployed at optimum locations in 3D space. However, the implementation of aerial BSs confronts various practical challenges. Unlike terrestrial base stations (BSs), which are almost always connected to the power grid, UAVs are powered by batteries. Therefore, one of these challenges is related to UAV power consumption and the development of feasible UAV recharge systems conquer in order to keep these aerial BSs operational. To address this challenge, researchers worked on different solutions to prolong the battery life in UAVs.

The overall amount of power used by the UAV consists of the electricity needed for the mechanical parts that are responsible for flight, as well as the power needed for communication with the users. Therefore, some researchers worked on reducing energy consumption in each of these parts.

Some approaches to reducing communication power consumption are written in the following. One feasible way to address this is to minimize the transmission power of one or multiple UAVs. In [34] and [35], it is shown that when the aerial base stations are placed in an optimal position where they can maximize the coverage in the target area, the required transmission power for one UAV or multiple UAVs is minimized, respectively. Authors in [36] addressed the problem of power minimization to meet the constraint of achieving the required for all ground users. In such a way, the optimization of UAVs' deployment was to minimize the overall transmit power. They also expressed that adjusting the UAVs' altitude to the optimal values besides using the optimal locations leads to minimum power consumption. Other work [37] derived the minimum number of stopping and transmission points for a UAV to cover all downlink users and shows that the reduction in the number of transmissions makes the energy consumption of UAVs decrease. To fulfill the demand for transmission power minimization, the researchers in [38] developed an optimum drone placement mechanism as a multi-objective optimization problem which was divided into two independent ones, one for each axis of movement; Horizontal positioning for minimization of distance sum and vertical positioning for maximization of coverage. In another work, the authors optimized the position and transmitted power separately by proposing a double-loop iterative algorithm to jointly optimize the transmit power and position of the UAV [21].

Although proposed approaches reduce the power needed for communication in UAVs, some researchers neglected the communication energy consumption of UAVs because it is much smaller than the energy needed for flying [39]. Therefore, while examining the energy efficiency of UAV communications, it is vital to also take the propulsion energy (mechanical part) consumption into account. To study the propulsion energy consumption in literature, some researchers suggest the UAVs' height as a key factor in reducing the energy consumption of propulsion. But altering the height may decrease the UAVs' performance. For instance, there is a tradeoff between energy consumption and coverage radius. Higher altitude leads to a higher radius but the propulsion energy consumption increases [40] [41]. The authors in [2] studied the energy efficiency of UAV communication by considering the optimization of flight radius and speed.

Besides reducing the power consumption of UAVs mentioned above, researchers have come up with other approaches to address the limited onboard energy of the UAVs. Their solution is to consider locations to replace the exhausted UAVs with fully charged ones. In [42], the proposed approach is to monitor the battery charge level of the UAVs by a Macro base station (MBS), and when it reaches a critical level, the MBS instructs the UAV to go back to the station for recharging, and the fully charged one is sent in its place. Also, in [40], the replacement of UAVs is suggested, and an optimization problem is formulated to minimize the number of required UAVs. To achieve energy-efficient communication, the authors in [43] presented a coverage model based on a multi-UAV system.

The aforementioned studies in the previous part did not investigate the advantages of energy harvesting for UAV-assisted wireless communications. The authors of [44] discussed using radio energy harvesting to increase the UAV's endurance period. In another study [45], they utilized energy harvesting technology to the UAV to save the electric power of the UAV's battery and increase flight endurance, where the gathered energy from the ground base station (GBS) is used as the transmit power of the UAV-assisted relay.

The mentioned approaches addressed the limited onboard energy by trying to optimize and decrease the energy consumption of the UAVs, and the preceding studies focused on energy harvesting via radio frequency sources rather than renewable energy sources.

Here, in this study, we are trying to address this issue by using solar energy to keep the UAV working and extend the endurance time.

### 3.3 Solar-Powered UAVs

In [46], the authors worked on a specific mid-class UAV system named Electrical Aerial Vehicle-2 (EAV-2) that consist of three types of power sources operating simultaneously: fuel cell, batteries, and solar cells. They study the data from the 22.13-hours test flight of the UAV with the objective of comprehending the performance characteristics of each power source and determining the viability of a hybrid electric power system. They also use power simulation to estimate the dynamic behavior of each power source and compare it with the flight test data, but their study was on a specific UAV and did not cover the other types of UAVs. Also, in [47], the improvement of flight performance and endurance in hydrogen fuel cell-PV power systems for small UAVs was studied. In another study [48], researchers provided a model of solar radiation intensity to simulate the solar cell's output power and designed and developed an energy monitoring system. The authors in [49] explored maximizing the total throughput for a solar-powered UAV system during a certain period. Although in all the mentioned studies, the simulation result based on their models was validated, they did not consider the solar forecast to predict the behavior of the UAVs.

In this study, we address the limited onboard energy of the UAVs by solar energy and by using the solar irradiance forecasting and simulating the energy consumption of the UAV, providing a simulation tool which can be used to predict the behavior of the solar-powered UAV which can play important role to planning and managing the operation of these UAVs.

## 4 Approach to Implementing the Simulator

In this section, we introduce an analytical tool that aims to provide information about the solar-powered UAV aerial base station to the practitioners by simulating the UAV and modeling the power consumption of the UAV, and using solar data forecast to predict the behavior and duration of providing service when it is used as the aerial base station.

In this chapter, first in 4.1, the components of the discrete-event simulator that we proposed in this study are explained. In the following section (Section 4.2), the energy consumption model of flying and communication of the UAV are described. When we talk about energy consumption, it is important to consider the storage of energy. Therefore, in Section 4.3, the model for the charging and discharging mechanism of the battery used in the UAV is explained. One of the most important parts of this study is the capability of the UAV to charge with solar energy harvesting, and the mechanism and procedure of it are mentioned in Section 4.4. Section 4.5 states the probabilistic solar irradiance forecasting and the ways that we can use it in our study. Last, in Section 4.6, we see the components that build our tool based on the inputs that we provide to the tool to run the simulation and the outputs that are the predicted information based on the mission scenario (Figure 4-1).

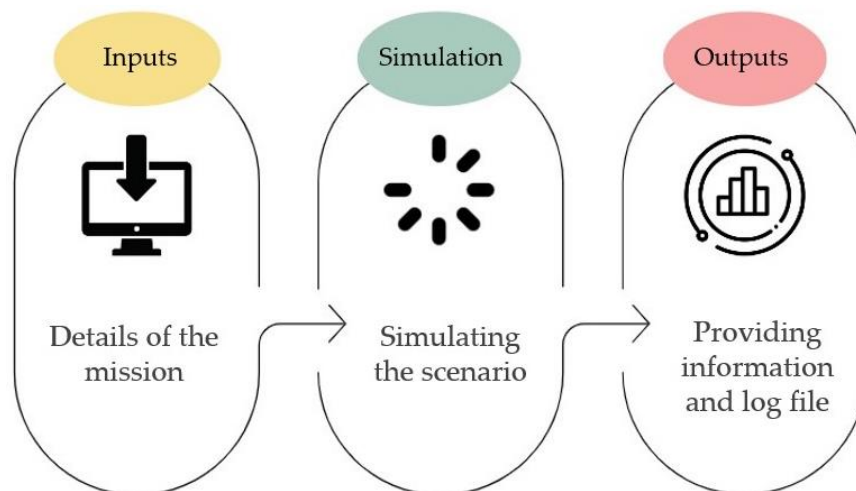


Figure 4-1: Components of the tool: In the inputs the operator provides the details such as the physical characteristics of the UAV and the distance to the area, and in the output the tool provides the information like the final status of the UAV and the predicted active time and battery charge level at the end of the simulation

## 4.1 Discrete-Event Simulation Components

In this section, the components and processes that should be supported by the anticipated tool are explained. The tool uses discrete event simulation, which is used to simulate real-world systems and has been discussed in Section 2.7. As it is explained in Section 2.7, this method of simulation works with a number of logically distinct processes that progress independently across time, and the state of each process can be changed by the occurrence of an event. In this section, we will discuss the different processes and events needed in the simulation of the solar-powered UAV and their interaction between these components. The summary of the processes is also shown in Figure 4-2.

### 4.1.1 Mission Monitor and Control Process

Mission control is a central process to monitor and coordinates the scenario-derived missions of the UAV. By having this unit, the UAV could be performed self-organized without an outside controller. The mission monitor and control unit is responsible for the behavior of the UAV and runs from the beginning until the end of the mission. When the UAV's battery reaches a certain threshold, it should go back to its initial station. Therefore, this unit should have knowledge about the goals and restrictions; also, it should be aware of the UAV's state during the missions to make the decision based on the goal and destination of the mission.

### 4.1.2 UAV State Process

The UAV state is dependent on the action and command that it receives from the mission monitor and control unit. The actions of the UAV consist of takeoff, landing, flying to/from the area of interest, hovering on top of the area of interest, or/and communicating with the users, and the needed energy by the UAV is measured based on its state. Each state has its own amount of energy consumption, which is explained in Section 0.

### 4.1.3 Battery Process

This process consists of UAV's battery behavior which charges or discharges itself based on the delta energy at each moment Equation (4-1). The delta energy ( $\Delta E$ ) is the difference between the harvested energy from the energy source and the needed energy for the UAV at the moment. If the consuming energy is more than the harvested energy, the battery discharges for the amount of delta energy; otherwise, it charges. The needed energy of the UAV is different in time based on the state of the UAV at each time step. The details about the charging and discharging model of the battery are explained in Section 4.3.

$$\begin{cases} \text{if } E_{harvested} > E_{needed} & \text{battery charges for } \Delta E \\ \text{if } E_{needed} > E_{harvested} & \text{battery discharges for } \Delta E \end{cases} \quad 4-1)$$

### 4.1.4 Interaction Between Processes

As mentioned above, the structure of the typical simulation is defined by three processes that have communication and coordination commands between themselves. As it is illustrated in Figure 4-3 when the mission starts, the monitor and control unit starts to observe the battery level of the UAV on a regular basis (every few time steps). If the battery level falls below the threshold, this unit commands the UAV to go back to its home station. At this moment, if the UAV's state is anything other than flying to the home station, the monitoring unit changes UAV's state to flying back home by using an event. On the other hand, at the beginning of the simulation, the UAV starts to fly towards the interested area, and when it reaches the destination, the state of the UAV is changed by an event to communicate. Moreover, the battery process charges and discharges the battery base on the UVS's state that takes from the UAV state process.

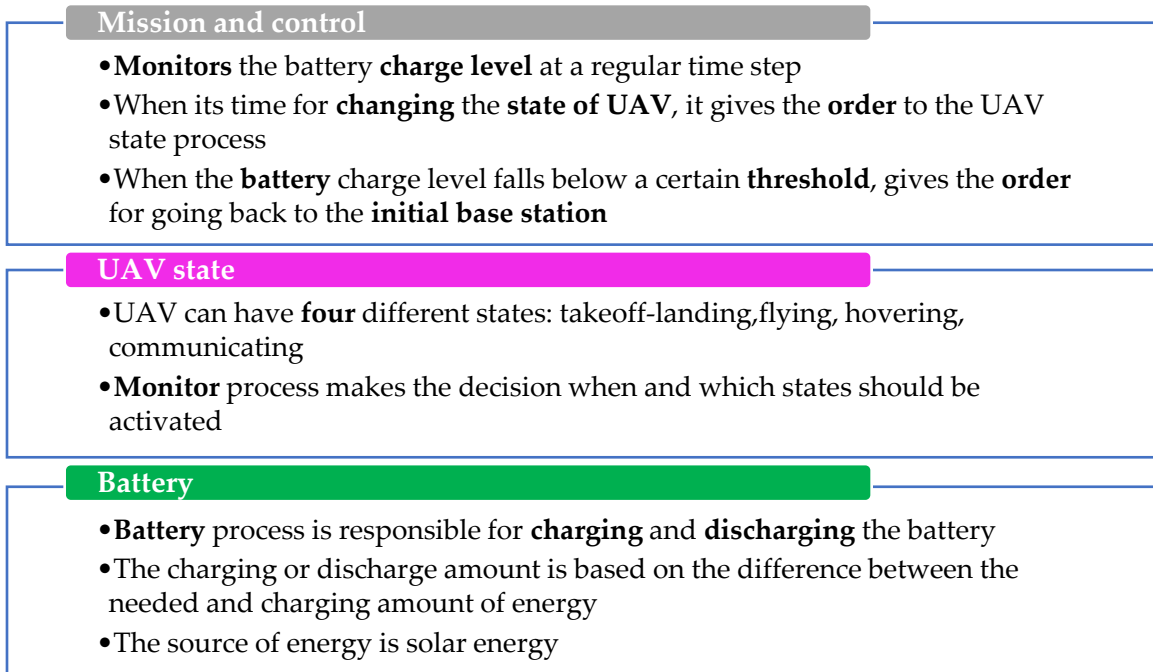


Figure 4-2: Processes used in the simulation

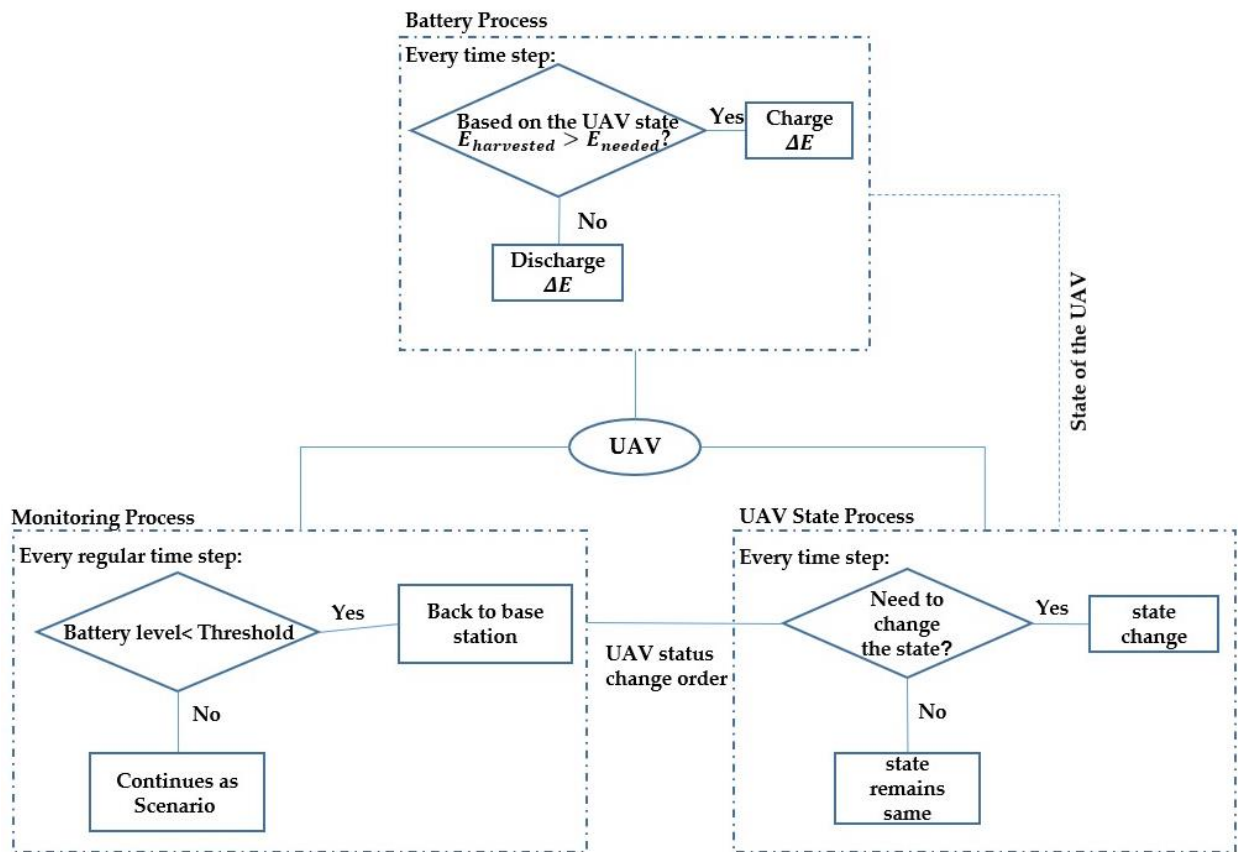


Figure 4-3: Connection between the processes

Figure 4-4 provides a high-level summary of the processes and their relative timing related to the scenario in evaluation scenario in Section 5.1.



Figure 4-4: Overview of processes using during the simulator from time point of view

## 4.2 UAV Energy Model

The model of flying energy consumption for the UAV is dependent on their mechanism of flying. Based on what was discussed in Section 2.2, the flying mechanism that is considered in this study is the UAV with the rotary-wings. Rotary-wing UAVs are able to takeoff and land vertically, and this ability makes them more suitable in the network providing cases where there is no human access place, and the UAV can land on a small area vertically. Also, the ability to hover of these UAVs is the most important point in situations where there is no landing place in the areas where the service is needed to provide by them. So the energy and power model that we consider in this study is related to rotary-wing UAVs.

The most important part of the simulation is the energy consumption of the UAV in different states of its mission. As it is shown in Equation (4-2), the total energy consumption of the UAV consists of the energy needed for mechanical parts related to flying and the energy required for communicating with the users.

$$E_t = E_{flying} + E_{comm} \quad (4-2)$$

We represent the fundamental equations for energy consumption in Section 2.4, designated as  $E$ , and the relevant units for clarity and ease of the energy model's exposition  $E[J]=Power[W]Time[s]$ . Therefore, to compute the energy consumed by a UAV to perform its mission, we designate that energy consumption is equal to the power needed for performing the task (flying or communicating) multiplied by the time spent doing the task.

In this section, we will study the needed energy and power model for flying and communication of the UAV in more detail.

### 4.2.1 Flying Energy Consumption Model

The flying energy consumption of UAV which can also be denoted as the energy needed for the electrical motors of UAV to perform Equation 4-3), is consisted of the energy used to lift the drone into the air until it reaches a hovering position referred to as takeoff energy, and the energy used to ground the drone properly is referred to as landing energy. The energy required to maintain the UAV's altitude, known as hovering energy, depends on both air properties, such as the UAV's mass and air density. The energy needed for movement is also the amount of (kinetic) energy needed to launch a drone from a hovering position.

$$E_{flying} = E_{takeoff} + E_{landing} + E_{hover} + E_{move} \quad (4-3)$$

It's interesting to note that, according to [45],  $E_{move}$  is just a multiplication constant that, when applied to a moving drone (in "normal" weather circumstances), slightly affect  $E_{hover}$ . Therefore, assuming that movement occurs under constant velocity, meaning that the energy contributed for stationary hovering is only a small portion of the energy consumed for movement. So, the simplification is considered in the total flying energy consumption:

$$E_{flying} = E_{takeoff} + E_{landing} + E_{hover} \quad 4-4)$$

To calculate the needed energy, we consider the power required for different components of rotary-wing UAVs. Induced power ( $P_I$ ), which creates thrust by directing air downward, profile power ( $P_p$ ), which counteracts the rotational drag of rotating propellers, and parasite power ( $P_{par}$ ), which mitigates body drag caused by the UAV's proximity to the wind, are three of the main components of rotary-wing UAV power consumption. The components are considered as expressed in [50]:

$$P_I(T, V_{vert}) = k_1 T \left[ \frac{V_{vert}}{2} + \sqrt{\left(\frac{V_{vert}}{2}\right)^2 + \frac{T}{k_2}} \right] \quad 4-5)$$

$$P_p(T, V_{air}) = c_2 \sqrt{T^3} + c_3 (V_{air} \cos \alpha_a)^2 \sqrt{T} \quad 4-6)$$

$$P_{par}(V_{air}) = c_4 V_{air}^3 \quad 4-7)$$

$$T = \sqrt{[mg - (c_5 (V_{air} \cos \alpha)^2)]^2 + (c_4 V_{air}^2)^2} \quad 4-8)$$

In the above equations,  $mg$  represents the UAV gravity,  $V_{vert}$  and  $V_{air}$  are vertical speed and horizontal air speed, respectively also  $T$  is the USV thrust which is expressed in Equation (4-8) and  $\alpha_a$  is the angle of attack.  $k_1$ ,  $k_2$ ,  $c_2$ ,  $c_3$ ,  $c_4$ ,  $c_4$  and  $c_6$  are related identified parameters which the values can be seen in Table 1, which is taken from [50].

Now, the power needed for hovering and takeoff/landing are expressed respectively as Equation(4-9) and Equation(4-10) [50]:

$$P_{hover} = P_I(mg, 0) + P_p(mg, 0) + P_{par}(0) = (c_1 + c_2)(mg)^{3/2} \quad 4-9)$$

$$P_{takeoff} = P_{landing} = P_I(mg, V_{vert}) + P_P(mg, 0) \quad 4-10$$

As it is shown in the above equations, the UAV gravity has an important role in the flying power consumption of the UAV. The consumed energy for UAVs with different weights is illustrated in Figure 4-5. And we have to consider that one of the factors that make a change in the weight of the UAV is the battery. As the capacity increases, the battery gets heavier and increases the weight of the UAV. (The energy consumption is reported in Wh and as it is mentioned in 2.4, 1Wh flying energy consumption is equal to 1 watt of power flow over the course of 1 hour flight)

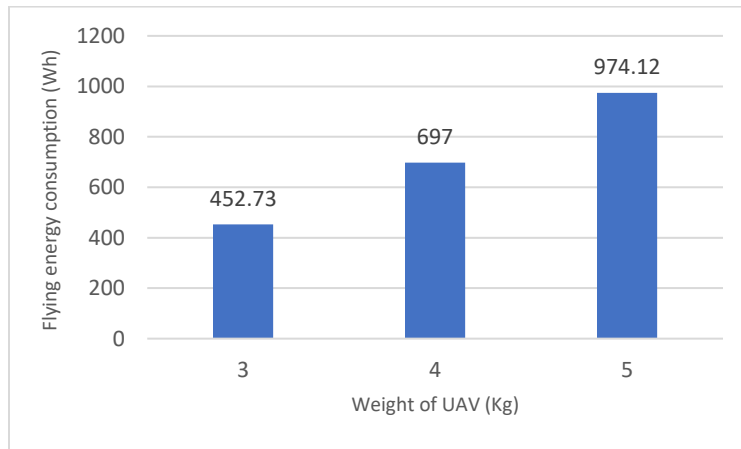


Figure 4-5: Flying energy consumption for different weights of UAV

| Parameter       | Value                 |
|-----------------|-----------------------|
| $k_1$           | 0.8554                |
| $k_2$           | $0.3051 (kg/m)^{1/2}$ |
| $c_1 = k_1/k_2$ | $2.8037 (m/kg)^{1/2}$ |
| $c_2$           | $0.3177 (m/kg)^{1/2}$ |
| $c_3$           | $\sim 0$              |
| $c_4$           | $0.0296 kg/m$         |
| $c_5$           | $0.0279 N s/m$        |
| $c_6$           | $\sim 0$              |

Table 1: Identified Parameters

## 4.2.2 Communication Energy Consumption Model

As mentioned in Section 3.2, in literature, the energy consumption of the communication part is neglected by some authors [2] [39] because it is much smaller compared to the flying energy consumption. However, in this study, we are concentrating on the total energy consumption of the solar-powered UAV and the network that it provides for ground users. In this way, it is essential to consider also communication energy consumption.

Based on what we discussed in Section 2.3, mmWave technology offers huge available bandwidth and multi-Gbps data rates. The short wavelength of mmWave signals allows multiple antenna elements to be placed into a small UAV. Moreover, massive MIMO can provide a very powerful beamforming system for a high number of antennas. In this study, I considered the use of HBF (hybrid beamforming) because, as mentioned in Section 2.3.2, besides its advantages, HBF consumes less power compared to ABF.

The communication power model that I used in this study is from [16], in which the power used by UAV during HBF transmissions is expressed analytically by the authors. Their concept takes into consideration the power used for communication by each electrical component, as is expressed in Equation (4-11).

$$P_{HBF} = P_{PA} + N_{RF}(2P_{DAC} + P_{RF} + P_{SP}) + N_T(N_{RF}P_{PS} + P_C) \quad 4-11$$

Where  $N_T$  is the total number of antenna elements,  $N_{RF}$  is the number of RF chains,  $P_{PA}$  is the power consumption of the power amplifier,  $P_{PS}$ ,  $P_{SP}$  and  $P_C$  are respectively represent power consumptions of the phase shifter, splitter, and combiner. The UAV is equipped with square Uniform Planar Arrays of  $N_T = N_X \times N_Y$  antennas. It uses  $N_{RF}$  RF chains ( $N_{RF} \leq N_T$ ) that produce  $N_D - 1$  tilted beam ( $N_D \leq N_{RF}$ ) besides the analog beam. For optimal deployment,  $N_D = N_{RF}$ .

Based on Equation (4-11), it is expected by increasing the number of antennas and RF chains, the energy consumption of communication increases. Figure 4-6 illustrates the communication power consumption of a UAV using different numbers of RF chains.

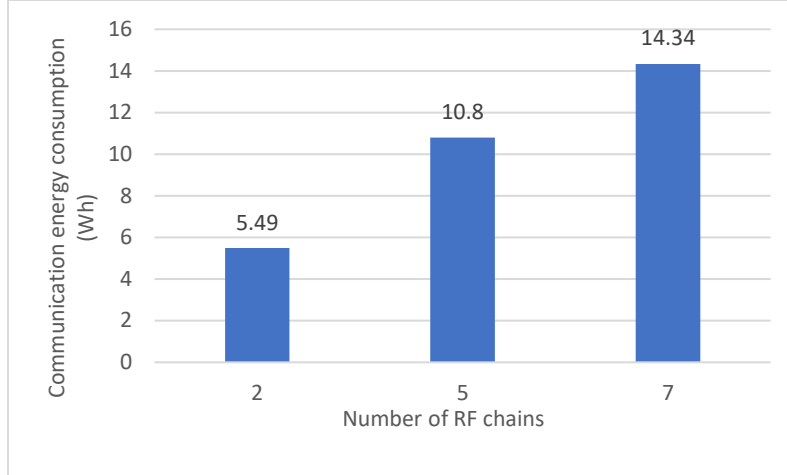


Figure 4-6: Communication energy consumption for different numbers of RF chains

### 4.3 Battery Charging/Discharging Model

Over the past decade, developments in energy storage have resulted in lithium-ion batteries (Li-ion) with great capacity and energy density. Li-ion batteries have the potential to be the primary energy storage in off-grid renewable energy. The main advantageous characteristics of Li-ion batteries are their longer lifetime than previous technologies, as well as their greater energy and power densities. The energy density of Li-ion batteries is usually 100-265 ( $Wh/Kg$ ). Li-ion has become a widespread, cost-effective storage medium for renewable energy as technology has progressed [51]. Li-ion batteries have a dynamic architecture and form factor that can accommodate complicated geometries. Li-ion batteries are already altering the automobile sector, and a similar transformation is anticipated in the UAV business [52]. For this reason, in this study, we consider Li-ion batteries to be implemented for the UAV.

We used the battery model that includes efficiency and linear charging/discharging rate limits with respect to the battery capacity C/L/C model from [53]. It explicitly models several characteristics of lithium-ion batteries, such as the limits on energy content, the loss of efficiency, and the limits on how much power can be applied in relation to the energy content.

$$b(k) = b(k - 1) + \Delta_E(k) \quad 4-12$$

$$\Delta_E(k) = \begin{cases} \bar{\eta}_c P(k) T_u & P(k) \geq 0 \\ \bar{\eta}_d P(k) T_u & P(k) < 0 \end{cases} \quad 4-13$$

$$\alpha_d V_{nom,d} \leq P(k) \leq \alpha_c V_{nom,c} \quad 4-14)$$

Equation (4-12) represents the battery energy content  $b(k)$  at the end of the time slot  $k$  or in other words,  $b(k)$  is the available amount of energy in the battery at the end of the  $k$ -th time slot. The duration of each time slot is  $T_u$ .  $n$  is the number of battery cells that are used, and Equation (4-13) shows the amount of charging/discharging energy based on the applied power  $P(k)$  in each time slot. It uses essential aspects of a battery cell, such as charging and discharging constant approximation efficiencies ( $\bar{\eta}_c$  and  $\bar{\eta}_d$ , respectively) and charging and discharging current limitations ( $\alpha_c$  and  $\alpha_d$ , respectively), which are transformed into power limits by multiplying them by the normal cell voltage ( $V_{nom,c}$  and  $V_{nom,d}$ )(see Equation(4-14)).

## 4.4 Solar Cell Harvesting Energy

The applied power of the battery can charge or discharge the battery. The source of the energy of the battery in this study is solar energy. To charge the battery using solar energy, as explained in Section 2.5, the suitable transducer for solar energy harvesting is photovoltaic (PV). The core component of a photovoltaic (PV) system is the solar cell which produces energy based on a number of variables, the most important of which is the amount of sunshine received during the daylight, called solar irradiance. Solar irradiance is the amount of power per unit area that comes from the sun as electromagnetic radiation in the range of the measuring device. The measurement of solar irradiance is per unit surface area ( $W/m^2$ ). Therefore, the amount of charging power for the battery, using solar power harvesting is, depended on the area of the solar cell. Moreover, the efficiency of the solar cells (the portion of solar energy that can be converted into electricity by the PV), which is a manufacturing characteristic of the solar cells, has an effect on the amount of harvested and produced energy for using by the UAV and charging the battery. Figure 4-7 shows the impact of the different efficiency and solar cell on the amount of harvested energy.

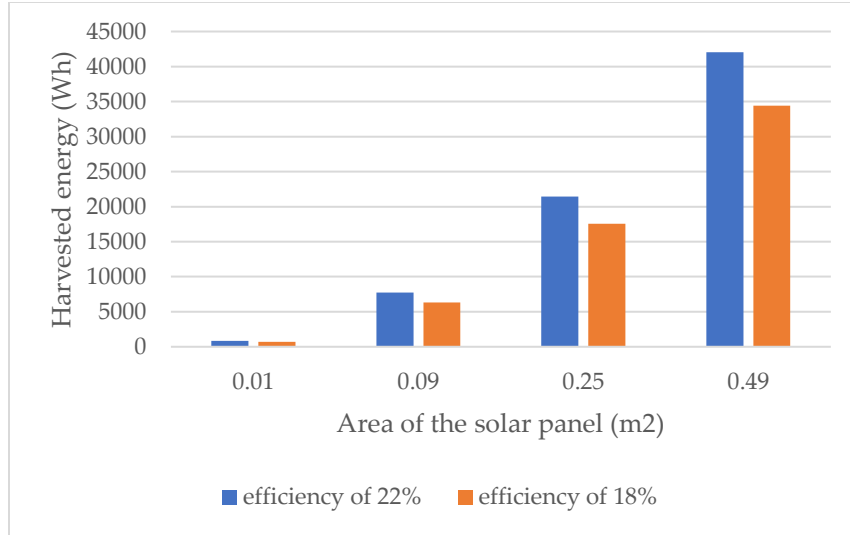


Figure 4-7: Amount of harvested energy with different sizes of solar panels and efficiency

In such a way, the amount of harvested energy using the PV can be expressed as Equation (4-15) where  $A_s$  and  $\eta_s$  are the area and the efficiency of the solar cells, respectively.  $I$  is the measured solar irradiance and  $T_u$  is the amount of time that the irradiance is measured for.

$$E_{harvested} = A_s \eta_s I T_u \quad 4-15)$$

For solar panels, the characteristics of Sunpower C60 photovoltaic were used. The advantages of Sunpower C60 are the anti-reflective coating and lower voltage and make each watt of power deliver an exceptional amount of energy to charge the battery. Their innovative all-back-contact design moves the gridlines to the back of the cell, which not only makes the cell more efficient (with maximum efficiency of 22%) but also makes it look better than other cells and makes it better for aerodynamic applications. Moreover, the light weight of this type of solar cell makes it a suitable candidate to use for UAVs because, as mentioned in Section 4.2.1, the weight of the UAV is an important factor in flying energy consumption. The specifications of the Sunpower c60 are written in Table 2: Weight and dimension of c60 solar cells.

| Parameter          | SI unit           |
|--------------------|-------------------|
| Mass of solar cell | 0.008 kg          |
| Length and width   | 0.125 m × 0.125 m |

Table 2: Weight and dimension of c60 solar cells

## 4.5 Probabilistic Solar Irradiance Forecasting

The most important part that differentiates this study is the ability of the provided tool to forecast the behavior of the UAV from the energy point of view by using probabilistic solar power forecasting. In such a way, by using probabilistic forecasting, we have the opportunity to choose whether the generated power from harvesting should depict a more optimistic or more pessimistic vision of the future. However, it is important to distinguish between two separate categories of probabilistic forecasting [54]. The first category is when the probabilistic forecast comprises the actual probability distribution for the solar power irradiance. In this case, we can predict the behavior of the UAV by simply randomly sampling from the distribution and getting the predicted produced power for each sample. Then by using the quantile function, we can determine how optimistic or conservating our prediction of the produced power using solar irradiance forecasting is. In the second situation, the distribution itself is not included in the prediction; instead, just the values for a set of quantiles (often the median with an upper and lower limit, such as the 10th and 90th percentiles) are provided. Since we cannot simply integrate the distribution, we offer an alternative approach. Based on the numbers of the pre-initialized quantiles, we can fit a proper distribution and get the sampling from the fitted distribution [55].

## 4.6 Tool Components

The tool represented in this study is designed to help the operators of the solar-powered UAVs to know how their drones will perform in their mission to provide a wireless network for the users by using different available equipment. In such a way, operators can give the details of the mission and the different available technologies they have to the tool, and the tool will simulate the mission of the UAV and the endurance time by using the power models and solar power forecasting. Therefore, it provides the vision for managing the mission of the UAV to provide a wireless network for the users. Each scenario would have its own characteristics, and each factor may play a more important role than the others. For example, in case of an emergency where the terrestrial BSs are down due to human or natural disasters, it is important that the UAV can stay active and provide coverage for the duration until the terrestrial BSs get recovered.

The tool gets the details of the mission from the operators and, by using the probabilistic weather forecast and power models and their components, simulates the behavior of the UAV and reports the final status and suitable information about the UAV so the operators can use this information for the important purposes such as risk assessments or comparing different equipment on the UAV. Moreover, since the tool can answer in a few minutes, so it is useful in case of an emergency where it is crucial to make the decision in a few seconds about how to equip the UAV for providing the wireless network in a specific area. In this chapter, the mechanism of the tool and its components (Figure 4-1) are expressed.

### 4.6.1 Input

The input of the tool is where the operator gives the details of the mission and each system component of the UAV to the tool. More specifically, the input of the tool is divided into three categories: model parameters, simulation data, and variables which are explained as follows. A summary of the input categories can be found in Figure 4-8.

| Model Parameters   | Simulation Data  | Variables   |
|--|--|---|
| <ul style="list-style-type: none"> <li>• Weight of the UAV</li> <li>• Average flying speed</li> <li>• Average landing/flying speed</li> <li>• Number of antennas</li> <li>• Number of RF chains</li> </ul> | <ul style="list-style-type: none"> <li>• The distance to the area of interest</li> <li>• The height that the UAV needs to ascent to</li> <li>• Start date and time of the simulation</li> <li>• Probabilistic solar irradiance forecast</li> </ul> | <ul style="list-style-type: none"> <li>• Maximum capacity of each battery</li> <li>• Available capacity of each battery</li> <li>• Weight of the of each battery</li> <li>• Threshold of each battery</li> <li>• Area of each solar panels</li> <li>• Efficiency of each solar panels</li> <li>• Weight of each solar panels</li> </ul> |

Figure 4-8: Input categories and the provided data by operator for each category

#### 4.6.1.1 Model Parameters

The model parameters are the inputs that are used in energy consumption models for flying and communication which are explained in Section 4.2, so the operator would determine the technical information of the UAV such as its weight, average flying speed and average landing/flying speed as well as the number of antennas and RF chains

needed to providing the wireless communications. In this way the tool can calculate the needed energy of the UAV in each step of it mission.

#### 4.6.1.2 Simulation Data

The simulation data are the inputs that are related to the outside of the UAV. In this part the operator gives the distance to the area of interest (where the UAV is needed to provide the service), the height that the UAV needs to ascent to it, start date and time of the simulation, and the probabilistic solar irradiance forecast for the twenty-four hours from the date and time that the UAV starts its task.

#### 4.6.1.3 Variables

Since the tool helps the operators to choose the best combination of equipment for the UAV based on the mission, the operators can give the different batteries and PV cells as the variables to the tool and provide discrete instantiations of variables. The details for each battery that we can give to the tool are its maximum capacity, available capacity (current energy level of the battery at the beginning of the mission), and weight of the battery. Another factor for the battery of the UAV is its threshold. This factor determines the battery energy level at which the UAV should go back to its initial station. The characteristics of the PV cells that users give to the simulation tool are their area, efficiency, and weight.

### 4.6.2 Simulation Process

The simulation process runs based on the inputs of the tool. In this way, the tool runs a number of experiments using the input information provided by the user and produces the outputs. The number of experiments is dependent on the number of batteries and solar cells provided in the variables part in inputs. For example, if the tool has 3 different batteries and 2 different PV available in input, it will run ( $3 \times 2 = 6$ ) experiments.

Each experiment consists of running the mission as a discrete-event simulation, explained in Section 4.1. The distance to the interested area that is provided in simulation data is used to estimate the time step that the UAV has reached the area of interest area and change the state of the UAV. The model parameters provided in the input are used to calculate the energy consumption of the flying and communication using the models provided in Section 4.2. The more important factor that is used in the simulation is

probabilistic solar irradiance. The two types of solar irradiance forecasting are mentioned in Section 4.5, and based on the type of it, we can get samples from the distribution of the forecasting. Since we are familiar with the initial distribution, we can evaluate our forecasts against the real event. In this way, each experiment runs for each sample and will send to outcome to predict the most probable situation of the UAV.

### 4.6.3 Output

The output of the tool provides information to the operators and practitioners to make a better-informed decision on how to equip the UAV considering its mission.

The output of the simulation consists of three metrics: 1) the most probable final status of the UAV, 2) the active time of the UAV during the simulation, and 3) the final battery level of the UAV at the end of the simulation. This information can be used to manage the operation and assess the risk of crashing the UAV.

Based on the battery capacity and available energy of it at the beginning of the simulation and the area of the available PV to charge the battery, the behavior of the UAV can defer in different combinations of battery and PV. The final status of the UAV defines how the tool predicts that the UAV will end its mission. There are three different final statuses for the UAV:

1. Providing service: This is when the UAV has successfully reached the destination of the mission, and at the end of the simulation, it is still providing the network to the users in the area of interest. This status is the preferable case because we know that the equipment and the battery threshold that we use for the UAV are good enough to keep the UAV alive all the time during the simulation.
2. Return to home (crashed/succeed): This is the status that the UAV has successfully reached the destination, but at a time step of the simulation, its battery charge level fell below the threshold, and it starts to go back to its initial station. The final battery level of the UAV can also report if the UAV has crashed before reaching the initial station or not. This status is somehow acceptable if the active time of the UAV during the simulation meets the requirement of the mission and doesn't crash before landing at the initial station.
3. Did not reach the destination: This is when the battery capacity, initial battery level, the available solar power and the battery threshold at the time of the simulation are not enough for the UAV to fly and reach the destination to provide

a wireless network. This status is the less preferable case because the UAV is not effective at all for the purpose that it is used, and it is highly probable if this setting of equipment is used on the UAV in the real world, it ends in the crash of the UAV.

Moreover, a log file of the simulation is provided, and it expresses the battery level and the status of the UAV at each time step in the monitor process, and it provides the UAV's step by step action based on the mission. Using the log file, the practitioners can find out what UAV is most probable to do in different states of its mission in a real event. For example, when the UAV climbs to the needed height when it starts to fly towards the destination, when it reaches the area of interest, and when it starts the communication and its battery level at each of these states.

# 5 Evaluation

To evaluate the tool and show its potential, a scenario of an emergency situation that aims to provide the network with a solar-powered UAV has been implemented by the tool. The results of the tool are presented and discussed in this section. First, we run the scenario with both energy harvesting and without energy harvesting to observe the different endurance time expansions. Moreover, different experiments are run based on the scenario to observe the outputs of them, and the outcomes with the probabilistic solar irradiance forecasting are compared with the real solar irradiance data to observe the proficiency of the tool.

## 5.1 Scenario setup

The experimental emergency situation scenario that was used for the evaluation of the tools is described in this section. The explanation of the scenario and its overview are provided in Section 5.1.1. In Section 5.1.2, the implementation of the scenario is explained, and the solar irradiance forecast and the way that we use it in our approach are written in Section 5.1.3.

### 5.1.1 Emergency Scenario

This scenario is based on an emergency situation in which the terrestrial base station in an area in the city of Berlin is down, and a UAV is needed to provide the wireless communication network in the same area. As it is mentioned in the literature in Section 3.2 and also can be observed by comparing Figure 4-5 and Figure 4-6, the energy consumption of flying is much higher than the energy needed for communication. In such a way, in this scenario, for having more duration of service by the UAV, we consider the UAV landing on an elevated area, such as a building, to perform its mission. So, the

scenario is as follows in detail and it is illustrated in Figure 5-1. When the mission starts, the solar-powered UAV starts to ascend from its initial station to an altitude; after it reaches the height, it starts to fly towards the emergency area as its destination. At the emergency area, it will land on a building; then, communication links will be established with the users. The UAV uses a MIMO antenna with mmWave and beamforming technology and NOMA multiple access. Moreover, a backhaul link is also considered using the IAB method. Then, whenever the battery level of the UAV falls below a threshold, the UAV should start to fly back to its initial station.

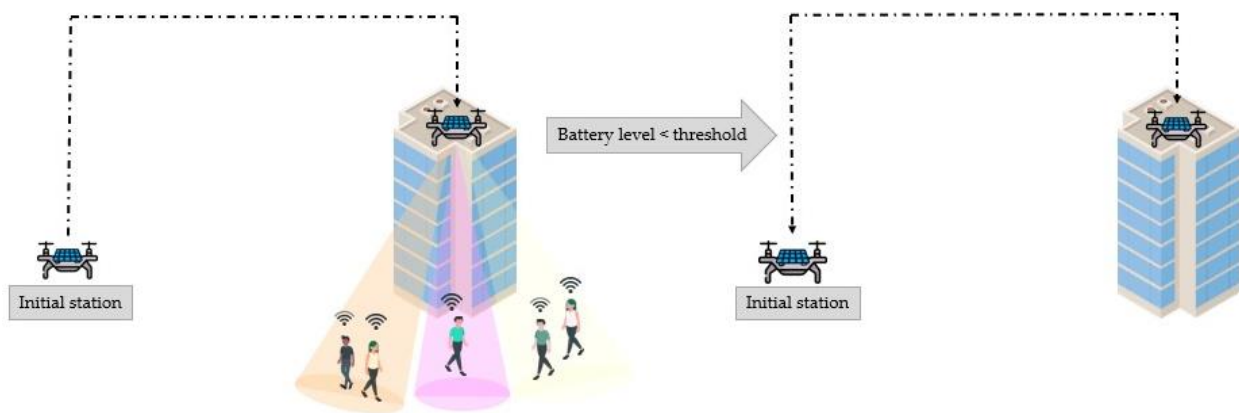


Figure 5-1: Overview of the scenario

### 5.1.2 Implementation of the Simulator

The tool is implemented in Python using SimPy. SimPy is a discrete-event simulation library written in Python. As it is explained in Section 2.7, discrete-event simulation works with a number of logically distinct processes that progress independently across time. In Simply, processes are used to represent the behavior of active components such as UAV in our scenario. Processes live in an environment and interact with the environment and with one another using events. Each process can produce events and then yield them to be triggered throughout their lifetime. When a process yields an event, SimPy suspends the process and resumes it when the event occurs (triggered). In SimPy, multiple processes can wait for the same event. Based on what is mentioned in Section 4.1, we use three different processes to simulate the behavior of the UAV as the aerial base station in the scenario. An overview of the processes and order of occurrence of the events are shown in Figure 4-4. It is important to note that the time step in this implementation is seconds. The monitoring process runs every 15 seconds and monitors the battery level of

the UAV. The battery process contains charging or discharging based on the energy consumption of the state of the UAV at each time step and charging based on solar irradiance forecasting. The UAV state is changed based on the order provided in the scenario, and the monitoring process orders the going back to the initial station based on the battery level and the threshold.

### 5.1.3 Solcast Probabilistic Forecasting

The available solar irradiance that we were able to use in this study was from Solcast [24]. Not every forecast has the same chance of being true, and different weather and climate conditions have a direct effect on how likely a forecast is to be right. Around a median forecast value, Solcast shows this uncertainty with confidence intervals that have a 10% and 90% chance of being true. The '10' possibilities show the forecast's lower bound of what is predicted (10<sup>th</sup> percentile). The '90' possibilities show the highest limit of what the prediction data forecasts (90<sup>th</sup> percentile). In this way, by using Solcast, we have the second type of probabilistic forecast mentioned in Section 4.5. Therefore, we needed to find a proper distribution to be able to fit it to the three percentiles provided by Solcast (10<sup>th</sup>, median and 90<sup>th</sup> percentiles).

Beta distribution is one of the distributions used to model the random fluctuation of solar irradiance, and this distribution has two parameters [56]. On the other hand, based on relative information we have from Solcast (only three percentiles), the three-point estimate approach is useful to generate an approximate probability distribution with three parameters for each distribution for best, most likely, and worst case estimation. PERT distribution is a transformation of the Beta distribution, which uses the three-point estimation. Therefore, by considering the three percentiles provided by Solcast, we decided to use the PERT distribution to fit. The three used parameters are the 10<sup>th</sup> percentile as the worst case, the median as the most likely, and the 90<sup>th</sup> percentile as the best case. By fitting this distribution in forecast data, we were able to generate samples aligned with the distribution and run the simulation many times (in this study, 100 times). By using these random samples, we can calculate and get the statistics for the output of the tool.

## 5.2 Experiment

Four experiments were conducted based on the mentioned scenario to study the impact of the different factors on the scenario. In the first experiment, the outputs of the scenario were compared in the case of using solar energy harvesting and the case that the battery is not charging. The second experiment shows the impact of the start time of the simulation and the initial battery level in the scenario. In the third experiment, we compare the results of the tool in both cases of solar irradiance forecast and real data, and the impact of battery threshold and start time, and the battery level was studied in both cases. The general use of the tool, which gives the ability to choose the best combination of the available equipment to the operators, is studied in the fourth experiment.

Some of the model parameters for the input of the tool are the same in all the experiments taken from [16] and can be found in Table 3. Moreover, the average ascending/descending velocity and average flying velocities are 2 *m/s* and 17 *m/s*, respectively, and the altitude of the UAV is 100 *m*, and all these inputs are also the same in all experiments. The average run time for each simulation with 100 samples on the solar irradiance forecast data is around 76s.

| Parameter        | Description             | Value                           | Parameter   | Description           | Value          |
|------------------|-------------------------|---------------------------------|-------------|-----------------------|----------------|
| $w$              | UAV weight              | 2.5 <i>kg</i>                   | $b_{DAC}$   | DAC bits              | 6              |
| $c_1 + c_2$      | UAV hovering parameters | $2.84 (m/kg)^{1/2}$             | $P_{LO}$    | Local oscillator      | 22.5 <i>mW</i> |
| $N_x \times N_y$ | Antenna array size      | [8*8]                           | $P_c$       | Combiner              | 19.5 <i>mW</i> |
| $P_t$            | Transmit power          | 24 dBm = 0.25 <i>W</i>          | $P_M$       | Mixer                 | 16.8 <i>mW</i> |
| $P_{PA}$         | Power amplifier         | $P_t/\epsilon, \epsilon = 27\%$ | $P_H$       | 90-deg hybrid coupler | 3 <i>mW</i>    |
| $P_{PS}$         | Phase shifter           | 21.6 <i>mW</i>                  | $P_{LPF}$   | Low pass filter       | 14 <i>mW</i>   |
| $P_{SP}$         | Splitter                | 19.5 <i>mW</i>                  | $P_{BBamp}$ | Base-band amplifier   | 5 <i>mW</i>    |
| $F_S$            | Sampling frequency      | 1 <i>GHz</i>                    |             |                       |                |

Table 3: Common parameters in all experiments

### 5.2.1 With and Without Energy Harvesting

In the first experiment, we ran the scenario in the implemented simulation to observe if using solar energy harvesting helps the extension of the active time of the UAV. In this way, we observed the active time of the UAV in both harvesting and not harvesting modes. The active time of the UAV refers to the amount of time that the UAV has enough battery to stay on. All the inputs are similar to each other, and both modes run for the same date and time. The solar irradiance data used in this experiment is the actual irradiance, not the forecast (this data is also provided by Solcast), and the solar panel is  $0.09 \text{ m}^2$  with 18% of efficiency. The destination of the mission is 5 Km away, the total capacity of the battery is 488 Wh, the battery level at the beginning of the simulation is 60% of the total capacity (292 Wh), and the threshold for the battery to get back to its initial station is set as 30 Wh. We planned the UAV to provide the network by using the 5 RF chains.

The experiment was run for five different start times of day (9 AM, 12 PM, 3 PM, 6 PM, and 10 PM) on 7<sup>th</sup> Jun 2022, and the operation time of the UAV was observed twenty-four hours from the start time. In all cases, the UAV returned to its initial station successfully. As it is shown in Figure 5-2, the outcome of total operation time for the scenario in the case of solar energy harvesting in all cases was higher. The difference between the two modes varies based on the start time of the simulation.

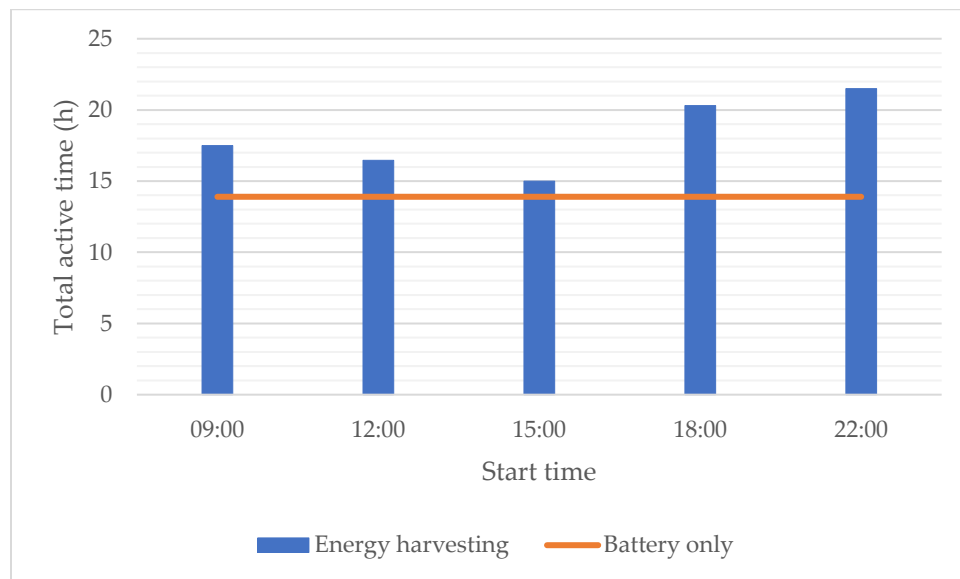


Figure 5-2: Comparison of using energy harvesting and only battery mode by UAV in the scenario

The amount of solar irradiance is illustrated in Figure 5-3, and as it can be seen, based on the different start times, the amount of harvested energy changes, and this factor can explain Figure 5-2.

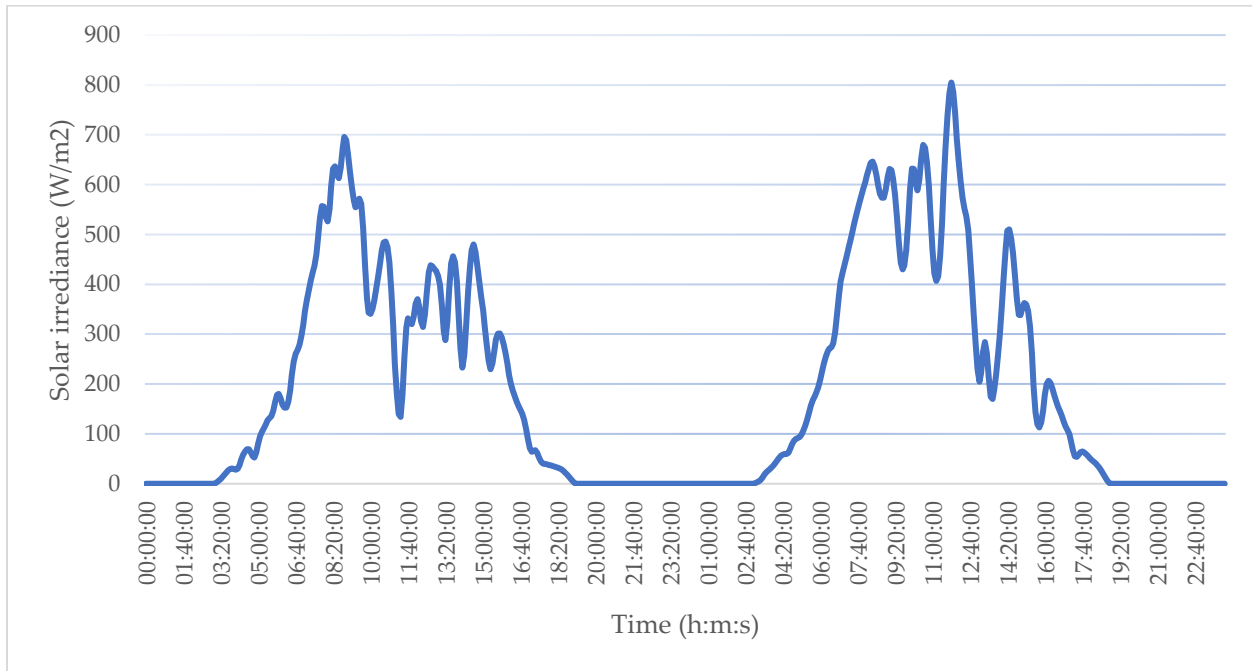


Figure 5-3: Solar irradiance for 24h after different start times

### 5.2.2 Different Start Times with Two Different Initial Battery Level

In this evaluation, we observed the prediction for the three main metrics of the simulation for the solar-powered UAV based on the scenario at the five different start times of the day like the previous evaluation (9 AM, 12 PM, 3 PM, 6 PM and 10 PM) on 7<sup>th</sup> July 2022 and different area for solar panels ( $0.04 m^2$ ,  $0.09 m^2$ ,  $0.16 m^2$  and  $0.25 m^2$ ) with the same efficiency of 18%. The total battery capacity of the UAV is 222 Wh, and the simulation was run for two separate initial battery levels of 100% and 60% (133 Wh) of the total capacity; the weight of the battery was considered as 1.5 kg, and the battery threshold for the battery for the going back to the initial station was set of 10% of the total capacity of the battery (22.2 Wh). The destination of the mission is 5 Km away from the initial station, and the 5 RF was used for providing the communication.

The three main parameters of the simulation (final status, service duration, and final battery level) for the battery fully charged at the beginning of the simulation are gathered in Figure 5-4. The best outcome for each start time is highlighted with green color, which means the best outcome for all three parameters is the result of using the biggest solar panel area.

The minimum active time of the UAV using different amounts of PV areas at different times of daylight is 12.48 hours. However, in simulations using solar panels with  $0.04 \text{ m}^2$  and  $0.09 \text{ m}^2$  area, the remaining battery level is less than 2% which could increase the risk of crash in these cases.

For the other simulation with the 60% battery level at the beginning of the experiment, as it is shown in Figure 5-5, all the cases have “return home” status with less than 2% remaining battery at the end of the simulation; this is the factor that can prevent the operator from using this kind of setting for the UAV. The minimum active time of the UAV in this setting will be 3.82 hours with the smallest solar panel area, which is 30.6% less than the same setting in the previous case, with a full charge battery at the beginning of the simulation. The maximum operation time for the UAV in the second battery setting is 16 hours. However, as mentioned before, the low amount of remaining batteries can cause uncertainty for the operators.

| PV area (m <sup>2</sup> )  | Start Time                | <br>9:00 | <br>12:00 | <br>15:00 | <br>18:00 | <br>22:00 |
|--|---------------------------|---|--|---|--|--|
|  | Parameters                |   |  |   |  |  |
| <br>0.04 m <sup>2</sup> | Remaining battery         | 1.35%   | 1.34%  | 1.30%   | 1.38%  | 1.42%  |
|  | Final Status              | Return home (successful)  | Return home (successful)   | Return home (successful)  | Return home (successful)   | Return home (successful)   |
|  | Predicted active time (h) | 14.26   | 13.32  | 12.62   | 12.48  | 14.8   |
| <br>0.09 m <sup>2</sup> | Remaining battery         | 1.34%   | 1.34%  | 1.36%   | 1.46%  | 1.36%  |
|  | Final Status              | Return home (successful)  | Return home (successful)   | Return home (successful)  | Return home (successful)   | Return home (successful)   |
|  | Predicted active time (h) | 16.60   | 14.64  | 13.11   | 13.01  | 20.23  |
| <br>0.16 m <sup>2</sup> | Remaining battery         | 17.56%  | 13.96%   | 14.0%   | 21.17%   | 21.63%   |
|  | Final Status              | Providing service   | Return home (successful)   | Return home (successful)  | Providing service  | Providing service  |
|  | Predicted active time (h) | 24  | 16.63  | 13.97   | 24   | 24   |
| <br>0.25 m <sup>2</sup> | Remaining battery         | 52.7%   | 54.5%  | 59.9%   | 59.78%   | 58.66%   |
|  | Final Status              | Providing service   | Providing service  | Providing service   | Providing service  | Providing service  |
|  | Predicted active time (h) | 24  | 24   | 24  | 24   | 24   |

Figure 5-4: Simulation outcome parameters for battery with full battery level





| PV area (m <sup>2</sup> )  | Parameters                | Start Time  |  |   |  |  |
|--|---------------------------|---|--|---|--|--|
|  |                           | <br>9:00 | <br>12:00 | <br>15:00 | <br>18:00 | <br>22:00 |
| <br>0.04 m <sup>2</sup> | Remaining battery         | 1.38%   | 1.36%  | 1.34%   | 1.35%  | 1.35%  |
|  | Final Status              | Return home<br>(successful)   | Return home<br>(successful)  | Return home<br>(successful)   | Return home<br>(successful)  | Return home<br>(successful)  |
|  | Predicted active time (h) | 5.43  | 4.77   | 4.18  | 3.82   | 3.80   |
| <br>0.09 m <sup>2</sup> | Remaining battery         | 1.36%   | 1.36%  | 1.35%   | 1.35%  | 1.35%  |
|  | Final Status              | Return home<br>(successful)   | Return home<br>(successful)  | Return home<br>(successful)   | Return home<br>(successful)  | Return home<br>(successful)  |
|  | Predicted active time (h) | 8.14  | 6.16   | 4.65  | 3.85   | 3.80   |
| <br>0.16 m <sup>2</sup> | Remaining battery         | 1.35%   | 1.35%  | 1.35%   | 1.35%  | 1.35%  |
|  | Final Status              | Return home<br>(successful)   | Return home<br>(successful)  | Return home<br>(successful)   | Return home<br>(successful)  | Return home<br>(successful)  |
|  | Predicted active time (h) | 11.8  | 8  | 5.31  | 3.88   | 3.80   |
| <br>0.25 m <sup>2</sup> | Remaining battery         | 1.35%   | 1.35%  | 1.35%   | 1.35%  | 1.38%  |
|  | Final Status              | Return home<br>(successful)   | Return home<br>(successful)  | Return home<br>(successful)   | Return home<br>(successful)  | Return home<br>(successful)  |
|  | Predicted active time (h) | 16  | 10   | 6.16  | 3.90   | 3.81   |

Figure 5-5: Simulation outcome parameters for battery with 60% of initial battery level

### 5.2.3 Predicted Outputs vs. Actual Outputs

This experiment contains the comparison of the output of the tool between the predicted and actual solar irradiance forecast, considering the different inputs to observe the performance of the tool and see how much our tool is reliable.

The three output parameters were observed for the solar-powered UAV with a total battery capacity of 488 Wh and an initial battery level of 292 Wh with 0.09 m<sup>2</sup> PV area on 7<sup>th</sup> July 2022. The observation simulation took place for different battery thresholds and different distances.

#### 5.2.3.1 Different Amounts of Threshold

The threshold is the main decision-making factor for the mission control process in simulating the operation of the UAV aerial base station in our study. At each step of battery level monitoring, whenever the battery charge level falls below the threshold, the UAV gets the order to go back home to its initial base station. In this experiment, we ran

the simulation for different amount of threshold for the start time of 12:00. The number of RF chains for communicating are 5.

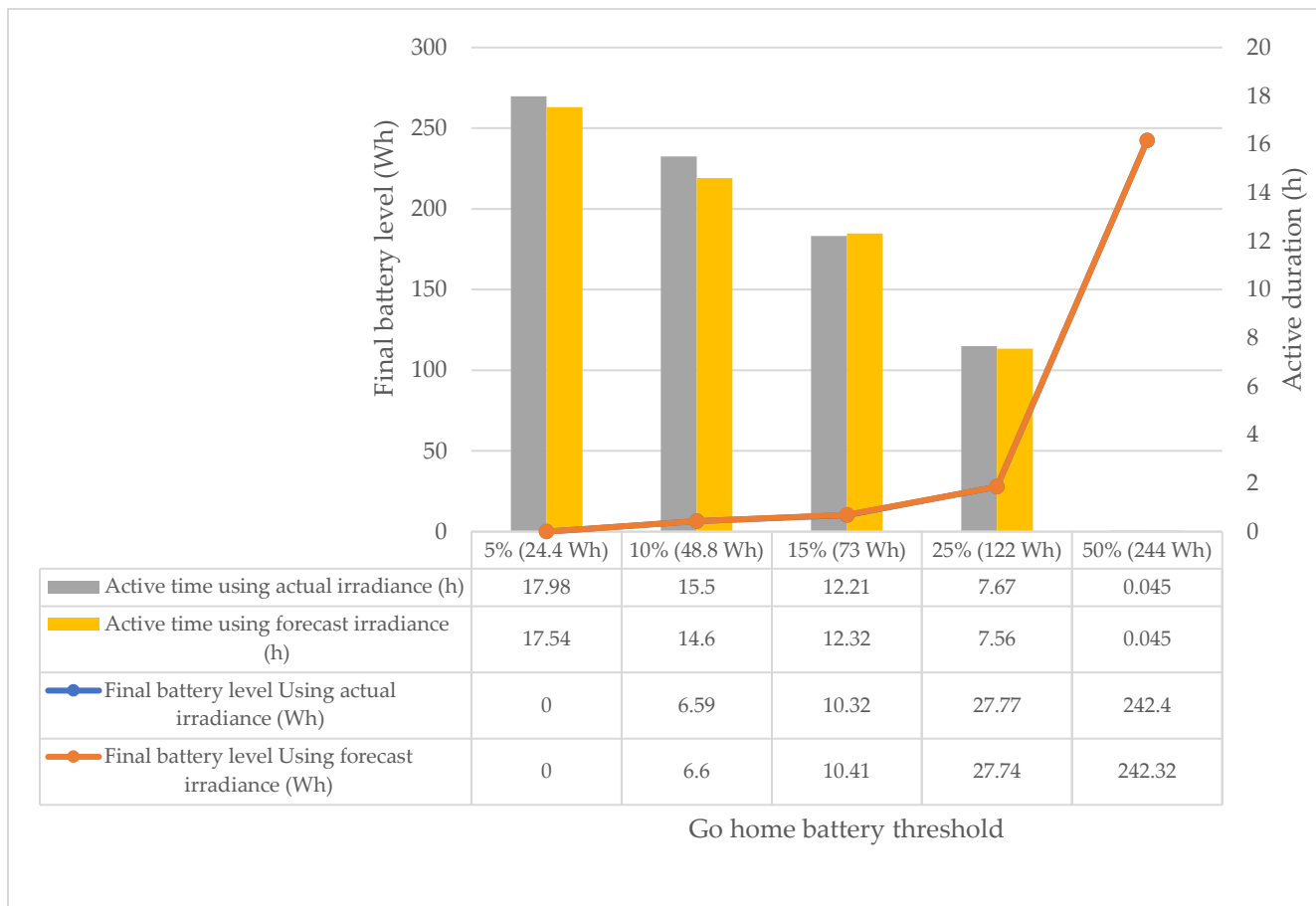


Figure 5-6: Active time and final battery level using actual and forecast solar irradiance for different amounts of battery thresholds

As can be seen in Figure 5-6, the final status outcome for the three intermediate thresholds (10%, 15%, and 20%) was successfully back to the initial station. They can be a good setting for the operation, considering the time that the UAV is needed to be active during the mission. For the simulation with the threshold of 5% of total capacity, although the active time of the UAV was around 14 hours in both predicted and actual irradiance data, the UAV status was crashed during flying back to the initial station, which is not the case that we want to happen for our equipment and UAV. On the other hand, the final situation of the simulation with the threshold of 50% showed that the UAV was not able to reach the operation destination and the active time of the UAV was less than 3 minutes, but the battery level was 242 Wh which can still make the UAV perform its mission. As we observed, choosing the threshold too high or too low can affect the operation

negatively; if the threshold is too low, it can cause the crash of the UAV, or if it's too high, the monitoring unit makes the UAV go back to the initial station too soon and the mission time will be much less than it should be.

### 5.2.3.2 Different distances to the mission destination

By increasing the distance of the mission area from the initial station, the UAV should fly for more amount of time, and this means more energy is needed to reach the destination. Consequently, the active time of the UAV during its mission will decrease by increasing the distance. To analyze the impact of the distance to the mission area on the main parameters of the simulation, we ran the tool in both actual and predicted modes for the destination areas in 5 km, 7 km, 9 km, and 11 km with the battery of he total capacity of

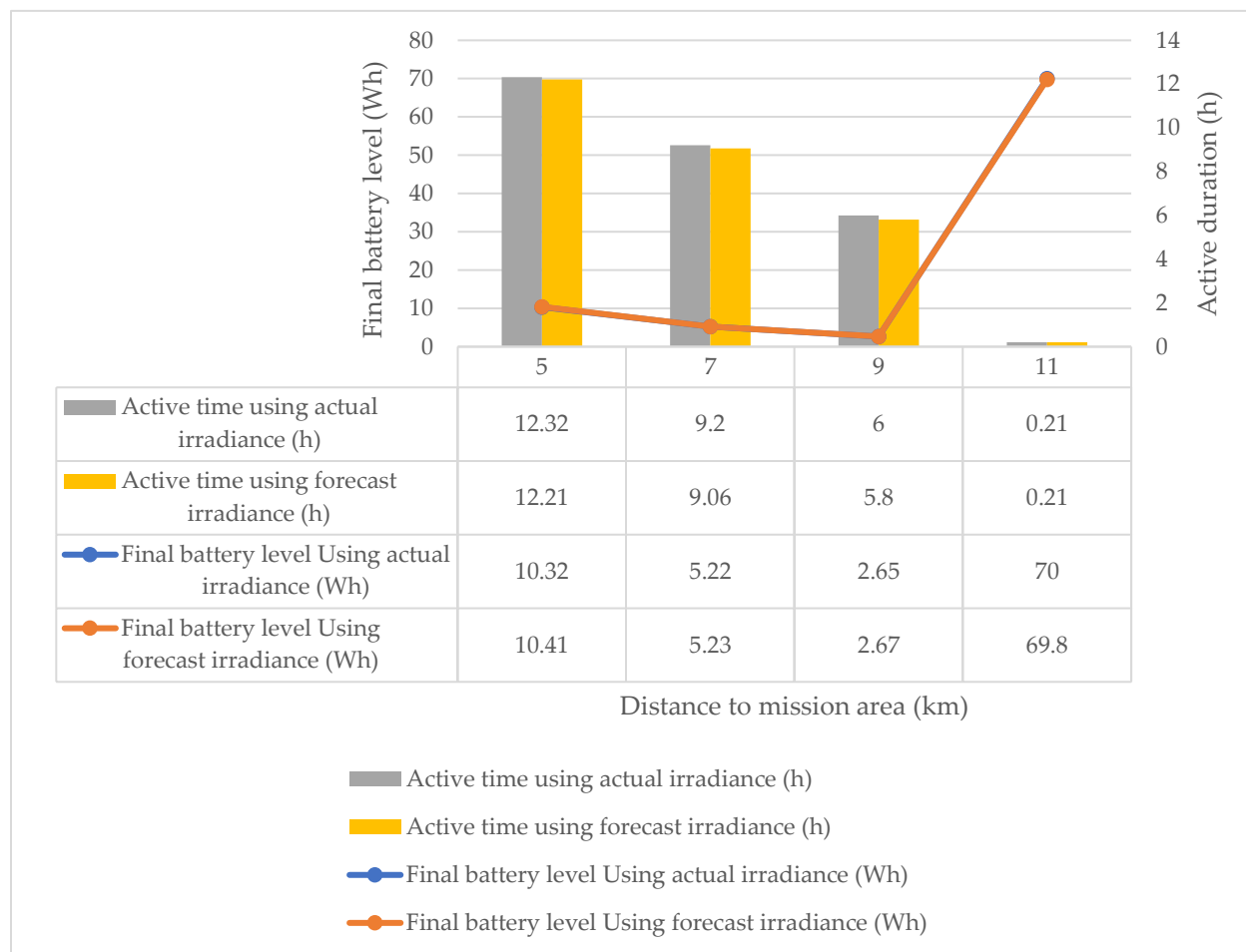


Figure 5-7: Active time and final battery level using actual and forecast solar irradiance for different distances to the mission area

488 Wh, with an initial battery level of 60% of the total capacity and a threshold of 15% (73 Wh). As it is shown in Figure 5-7, the changes in active time of the UAV were as we expected for the three first observations (5, 7, and 9 km), and the final status of them were all back to station successfully, but for the destination 11 km from the initial station, the destination was too far for the UAV to be able to reach. In this way, the distance to the area is also a factor that the tool can help the operators of the solar-powered UAV to decide on the mission base on the available equipment.

By comparing the outputs in two forecasts and actual solar irradiances, we can see that the tool works perfectly to help the operators. However, the probabilistic solar irradiance forecast that we got from Solcast only provides three percentiles of the distribution of the solar irradiance, and this may decrease the quality of the input forecast data to the tool. But at the moment of doing this study, Solcast was the available data to use in our study. Using the data, which covers most of the distribution, will increase the quality of the forecast.

#### 5.2.4 Using Different Equipment

To see the performance of the tool to provide insight to the practitioners as to how they can equip their solar-powered UAV as an aerial base station when they have different settings for battery and solar panel, in this experiment, we ran the tool for two different solar panels and three different batteries. Both solar panels have 18% of efficiency, one of them has  $0.09 \text{ m}^2$  PV area, and the second one has an area of  $0.04 \text{ m}^2$  (Table 4).

|       | Area (m <sup>2</sup> ) | Efficiency |
|-------|------------------------|------------|
| PV #1 | 0.09                   | 18%        |
| PV #2 | 0.04                   | 18%        |

Table 4: Information on the solar cells used in the experiment

The input information about the three batteries is written in Table 5.

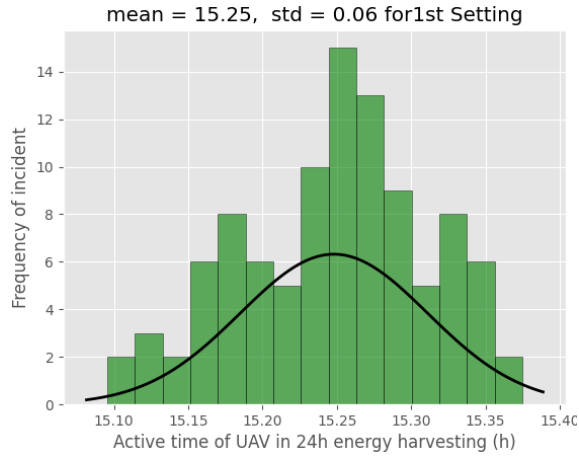
|            | Total capacity (Wh) | Initial battery (Wh) | Threshold |
|------------|---------------------|----------------------|-----------|
| Battery #1 | 222                 | 222                  | 10%       |
| Battery #2 | 488                 | 244                  | 15%       |
| Battery #3 | 488                 | 400                  | 50%       |

Table 5: Information on the batteries used in the experiment

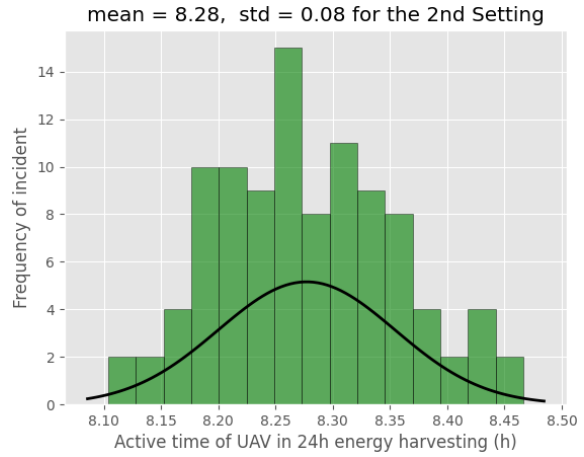
All the possible combinations of the solar cells and the batteries are considered as the equipment of the UAV in the defined scenario and used by the tool for the 8<sup>th</sup> of July 2022 for the start time of 12:00, and the operation is for a 5 km distance. For each combination, the tool tells the most probable final status and final battery level. Moreover, for the active time of the UAV, it provides a histogram chart that expresses the frequency of the active time as the output of the 100 random samples from the forecast solar irradiance, and we fitted a gaussian distribution on the chart. In such a way, the practitioners can manage the mission based on the active time they want for the operation. Also, the log file provides the start and finish time steps of the actions of the UAV. Table 6 shows the summary of the predicted outputs of the different settings of the equipment and based on the insight that the log file provides, they can manage the operation based on how long they want to provide communication in the area.

For the first combination (PV #1 and Battery #1), the tool predicts that the UAV will return successfully to its initial station, and the final battery level will be around 3 Wh. From the log file, we understand the UAV was in communication mode for 14.8 hours on average, and the chart for the active time can be found in Figure 5-8(a), with a mean value of 15.25 hours and a standard deviation of 0.07 and the tool can 90% guarantees the minimum 15.15 hours of active time with final status of returning home for the first setting.

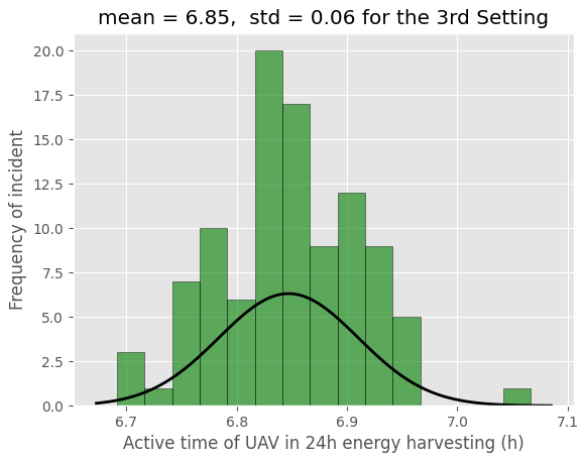
The same observation took place for PV #1 and Battery #2 as the second set. Also, in this setting is predicted that the UAV will return home successfully, and the remaining battery level is around 10 Wh. Figure 5-8 (b) represents the chart for this setting, and the UAV's active time is predicted to be 8.28 hours on average. The information for the other settings is also illustrated in Figure 5-8. Having the information for the fitted gaussian distribution and the remaining battery would help the operators to manage the risk of crashing the UAV.



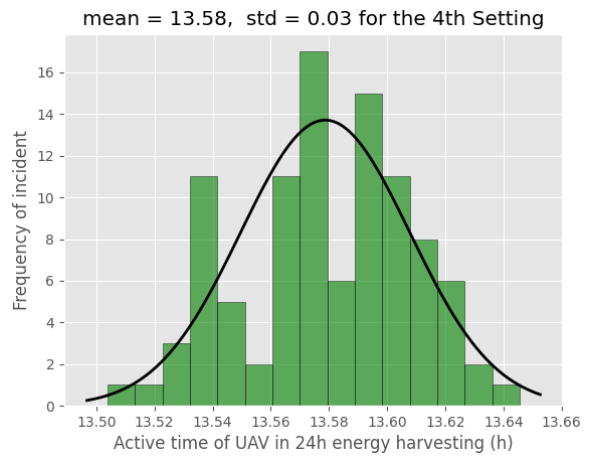
(a)



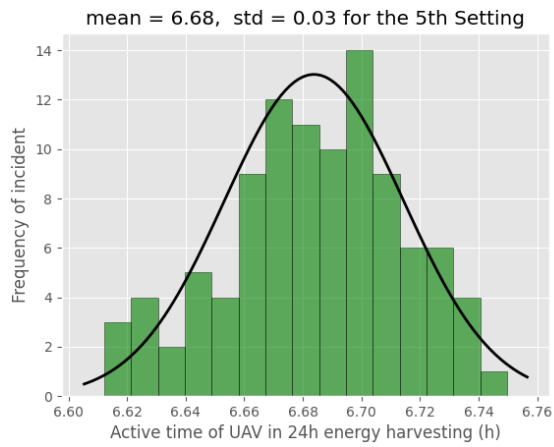
(b)



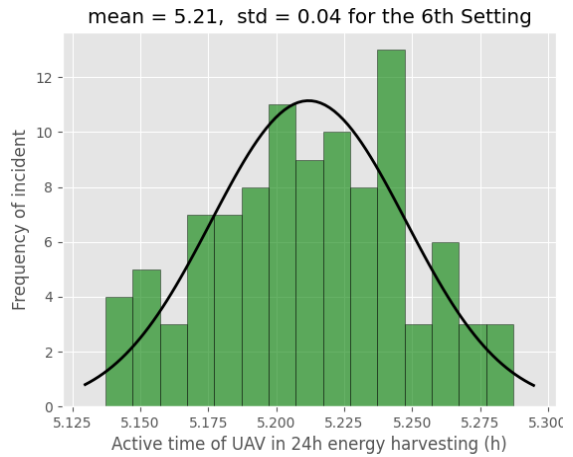
(c)



(d)



(e)



(f)

Figure 5-8: Histogram and fitted gaussian distribution on the output of the samples for the active time of the UAV

|                   | Number of settings | Final status             | Average remaining battery (Wh) | Average communication duration (h) |
|-------------------|--------------------|--------------------------|--------------------------------|------------------------------------|
| PV #1, Battery #1 | #1                 | Return home (successful) | 3                              | 14.8                               |
| PV #1, Battery #2 | #2                 | Return home (successful) | 10.3                           | 8                                  |
| PV #1, Battery #2 | #3                 | Return home (successful) | 143                            | 6.5                                |
| PV #2, Battery #1 | #4                 | Return home (successful) | 2                              | 13                                 |
| PV #2, Battery #2 | #5                 | Return home (successful) | 9                              | 6.2                                |
| PV #2, Battery #3 | #6                 | Return home (successful) | 139                            | 4.8                                |

*Table 6: Predicted outputs for the six different solar cells and battery settings*

One important point that should be considered in the experiments is that the available solar irradiance forecasting was available for us in this study was the Solcast data, and it contained only three percentiles of the distribution, which led us to use PERT distribution to get the samples for the simulation from it, which the information on the distribution with only three percentiles, can affect the quality of the outcomes negatively. Moreover, we did not have information on temporal interdependencies.

## 6 Conclusion and Future Work

This study set out to implement an analytical tool to help the operators to manage and equip a solar-powered UAV as an aerial base station. Coming up with solar-powered UAVs and using solar power harvesting is an answer to the limited onboard energy of the UAVs to extend their endurance time. However, the amount of harvested power underlies some uncertainty due to variability of solar power, and this makes it hard for the practitioners to manage and equip the solar-powered UAV for operation based on its details. Our tool uses the discrete-event simulation to simulate the behavior of the solar-powered UAV as an aerial base station during its mission from the energy point of view by adopting the details of the mission and probabilistic solar power forecast. There are many factors that have an impact on the performance and duration that the UAV can perform its mission, such as the battery threshold that the UAV must leave the mission area gets back to its initial station safely or the initial battery threshold and the start time of the mission can have an impact on the duration. There are three main parameters as the outputs of the simulation tool, which are the predicted active time of the UAV in its mission, the final status of the UAV, and the final battery level at the end of the simulation. Moreover, the tool also produces a log file that expresses the actions and state of the UAV at the different time steps. The provided information by the tool helps the operators to decide and manage the mission of the UAV more confidently.

To evaluate the capability of the simulation tool, we did four different experiments on a scenario in which a UAV has to fly towards an emergency area and provide the network to ground users after it lands on an elevated area. The average time for the tool to perform the simulations, was on average 76 second. This average execution time can aid the operators to access the information about the mission of the UAV on average less than two minutes. The available solar irradiance data for us in this study was Solcast. We used the actual and probabilistic solar irradiance forecast to perform the experiments on the tool and by comparing the outcomes of the simulator for both predicted and actual outcomes, the experiment showed a maximum 5% difference between the two cases. We also observed the extension operation duration with and without the energy harvesting capacity. Then we study the impacts of the different inputs, such as start time, threshold, and distance of the mission area, on the outputs. However, the forecast irradiance

provided by Solcast contains the three percentiles and doesn't contain all the irradiance distribution and the temporal dependency. Having better quality solar irradiance data will increase the tool's performance.

Our study contains the simulation and implementation of one UAV. Moreover, this simulator allows for extensions of the scenarios with more discrete events, such as reducing the energy used in the communication part or landing the UAV on a different station at the end of the simulation. All the mentioned capabilities of our simulator such as small run time, high accuracy and flexibility to simulate different scenarios make it an excellent tool to manage and predict the operation of the solar-powered UAVs as aerial base stations. For future studies, this study can be extended to simulate more than one UAV to be able manage and plan a group of UAVs to provide the network. By having more than one UAV it is possible to cover a wider area and more number of ground users and the networking of these UAVs would bring interesting research topics to extend this research and provide more useful information to the operators.

# List of Figures

|  |    |
|--|----|
| Figure 2-1: Adopted from [5], Figure5. propulsion power consumption vs. UAV flying speed: a) Fixed-wing UAVs b) Rotary-wing UAVs .....   | 6  |
| Figure 2-2: Adopted from [16], Figure3. HBF architecture with multiple RF chains.....  | 9  |
| Figure 2-3: From [60], downlink NOMA .....   | 11 |
| Figure 2-4: Potential IAB network for UAV aerial base stations.....  | 11 |
| Figure 2-5: Basic components of an energy harvesting system.....   | 13 |
| Figure 4-1: Components of the tool: In the inputs the operator provides the details such as the physical characteristics of the UAV and the distance to the area, and in the output the tool provides the information like the final status of the UAV and the predicted active time and battery charge level at the end of the simulation ..... | 20 |
| Figure 4-2: Processes used in the simulation .....   | 22 |
| Figure 4-3: Connection between the processes .....   | 23 |
| Figure 4-4: Overview of processes using during the simulator from time point of veiw   | 23 |
| Figure 4-5: Flying energy consumption for different weights of UAV .....   | 26 |
| Figure 4-6: Communication energy consumption for different numbers of RF chains...   | 28 |
| Figure 4-7: Amount of harvested energy with different sizes of solar panels and efficiency .....   | 30 |
| Figure 4-8: Input categories and the provided data by operator for each category.....  | 32 |
| Figure 5-1: Overview of the scenario .....   | 37 |
| Figure 5-2: Comparison of using energy harvesting and only battery mode by UAV in the scenario .....   | 40 |
| Figure 5-3: Solar irradiance for 24h after different start times .....   | 41 |
| Figure 5-4: Simulation outcome parameters for battery with full battery level .....  | 43 |
| Figure 5-5:Simulation outcome parameters for battery with 60% of initial battery level   | 44 |

|   |    |
|---|----|
| Figure 5-6: Active time and final battery level using actual and forecast solar irradiance for different amounts of battery thresholds..... | 45 |
| Figure 5-7:Active time and final battery level using actual and forecast solar irradiance for different distances to the mission area.....  | 46 |
| Figure 5-8: Histogram and fitted gaussian distribution on the output of the samples for the active time of the UAV .....                    | 49 |

# List of Tables

|   |    |
|---|----|
| Table 1: Identified Parameters .....  | 26 |
| Table 2: Weight and dimension of c60 solar cells.....                                   | 30 |
| Table 3: Common parameters in all experiments.....                                      | 39 |
| Table 4: Information on the solar cells used in the experiment .....                    | 47 |
| Table 5: Information on the batteries used in the experiment.....                       | 48 |
| Table 6: Predicted outputs for the six different solar cells and battery settings ..... | 50 |

## Bibliography

- [1] L. Godage, "Global Unmanned Aerial Vehicle Market (UAV) Industry Analysis and Forecast (2018--2026)," *Montana Ledger*, 2019.
- [2] Yong Zeng; Rui Zhang, "Energy-Efficient UAV Communication With Trajectory Optimization," *IEEE Transactions on Wireless Communications*, Vols. 16, no. 6, p. 3747–3760, Jun 2017.
- [3] S. Hayat, E. Yanmaz and R. Muzaffar, "Survey on Unmanned Aerial Vehicle Networks for Civil Applications: A Communications Viewpoint," *IEEE Communications Surveys & Tutorials*, vol. 18, no. 4, pp. 2624 - 2661, 2016.
- [4] X. You, C. Wang, J. Huang, X. Gao, Z. Zhang, M. Wang and Y. Huang, "Towards 6G wireless communication networks: Vision, enabling technologies, and new paradigm shifts," *Science China Information Sciences*, 2021.
- [5] X. Jiang, M. Sheng, N. Zhao, C. Xing, W. Lu and X. Wang, "Green UAV communications for 6G: A survey," *Chinese Journal of Aeronautics*, May 2021.
- [6] S. Sekander, H. Tabassum, E. Hussain,, "Statistical Performance Modeling of Solar and Wind-Powered UAV Communications," *IEEE Transactions on Mobile Computing*, Vols. 20, no. 8, pp. 2686-2700, Aug. 2021.
- [7] P. Oettershagen, A. Melzer, T. Mantel, K. Rudin, T. Stastny, B. Wawrzacz and T. Hinzmann, "Perpetual flight with a small solar-powered UAV: Flight results,

- performance analysis and model validation," *IEEE Aerospace Conference*, pp. 1-8, 2016.
- [8] M. Xiao, S. Mumtaz, Y. Huang, L. Dai, Y. Li, M. Matthaiou, G. K. Karagiannidis, E. Björnson, K. Yang, C.-L. I. and A. Ghosh, "Millimeter Wave Communications for Future Mobile Networks," *IEEE Journal on Selected Areas in Communications*, vol. 35, p. IEEE Journal on Selected Areas in Communications, 2017.
- [9] Y. Zeng, R. Zhang and T. j. Lim, "Wireless communications with unmanned aerial vehicles: Opportunities and challenges," *IEEE Communications magazine*, pp. 36-42, 2016.
- [10] A. FOTOUHI, H. QIANG, M. DING, H. MAHBUB, L. GIORDANO, A. Garcia-Rodriguez and J. Yuan, "Survey on UAV Cellular Communications: Practical Aspects, Standardization Advancements, Regulation, and Security Challenges," *IEEE Communications Surveys & Tutorials*, pp. 3417-3442, 2019.
- [11] Y. Zeng, J. Xu and R. Zhang, "Energy Minimization for Wireless Communication With Rotary-Wing UAV," *IEEE Transactions on Wireless Communications*, pp. 2329-2345, April 2019.
- [12] Q. Wu, L. Liu and R. Zhang,, "Fundamental Trade-offs in Communication and Trajectory Design for UAV-Enabled Wireless Network," *IEEE Wireless Communications*, Vols. 26, no.1, pp. 36-44, February 2019.
- [13] M. Mozaffari, W. Saad, B. Bennis, Y.-H. Nam and M. Debbah, "A Tutorial on UAVs for Wireless Networks: Applications, Challenges, and Open Problems," *IEEE communications surveys & tutorials*, pp. 2334-2360, 2019.
- [14] A. Sawalmeh, N. S. Othman and H. Shakhathreh, "Efficient Deployment of Multi-UAVs in Massively Crowded Events," *Sensors*, 2018.
- [15] X. Cao, P. Yang, M. Alzenad, X. Xi, D. Wu and H. Yanikomeroglu, "Airborne communication networks: A survey," *IEEE Journal on Selected Areas in Communications*, 2018.

- [16] Y. Wang, M. Giordani, X. Wen and M. Zorzi, "On the beamforming design of millimeter wave UAV networks: Power vs. capacity trade-offs," *Computer Networks*, 2022.
- [17] Z. Xiao, L. Zhu, Y. Liu, P. Yi, R. Zhang, X.-G. Xia and R. Schober, "A survey on millimeter-wave beamforming enabled UAV communications and networking," *IEEE Communications Surveys & Tutorials*, pp. 557-610, 2021.
- [18] I. Ahmed, H. Khammari, A. Shahid, A. Musa, K. S. Kim, E. De Poorter and I. Moerman, "A survey on hybrid beamforming techniques in 5G: Architecture and system model perspectives," *IEEE Communications Surveys & Tutorials*, 2018.
- [19] W. Belaoura, K. Ghanem, M. z. Shakir and M. O. Hasna, "Performance and User Association Optimization for UAV Relay-Assisted mm-Wave Massive MIMO Systems," *IEEE Access*, vol. 10, pp. 49611 - 49624, 2022.
- [20] Z. Ding, X. Lei, G. K. Karagiannidis, R. Schober, J. Yuan and V. K. Bhargava, "A survey on non-orthogonal multiple access for 5G networks: Research challenges and future trends," *IEEE Journal on Selected Areas in Communications*, vol. 35, pp. 2181-2195.
- [21] X. Jiang, Z. Wu, Z. Yin, Z. Yang and N. Zhao, "Power consumption minimization of UAV relay in NOMA networks," *IEEE Wireless Communications Letter*, 2020.
- [22] S. Chalasani and J. M. Conrad, "A survey of energy harvesting sources for embedded system," in *IEEE SoutheastCon*, IEEE, 2008, pp. 442--447.
- [23] P. Visconti, P. Primiceri, R. Ferri, M. Pucciarelli and E. Venere, "An overview on state-of-art energy harvesting techniques and choice criteria: a wsn node for goods transport and storage powered by a smart solar-based eh system," *Int. J. Renew. Energy Res*, 2017.
- [24] "<https://solcast.com/>," [Online].
- [25] E. Babulak and M. Wang, Discrete event simulation, InTech, 2010.

- [26] A. Mayer, "<https://www.x-plane.com/>," [Online].
- [27] A. R. perry, "The flightgear flight simulator," *Proceedings of the USENIX Annual Technical Conference*, 2004.
- [28] "[https://dev.px4.io/v1.10\\_noredirect/en/](https://dev.px4.io/v1.10_noredirect/en/)," [Online].
- [29] s. shah, d. debadeptha, l. chris and k. ashish, "Airsim: High-fidelity visual and physical simulation for autonomous vehicles," in *Field and service robotics*, 2018, pp. 621--635.
- [30] M. Mueller, V. Casser, J. Lahoud, N. Smith and B. Ghanem, "Ue4sim: A photo-realistic simulator for computer vision applications," *arXiv*, 2017.
- [31] F. De Rango, N. Palmieri, A. F. Santamaria and G. Potrino, "A simulator for UAVs management in agriculture domain," *International Symposium on Performance Evaluation of Computer and Telecommunication Systems*, 2017.
- [32] E. A. Marconato, M. Rodrigues, R. d. M. Pires, D. F. Pigatto, A. R. Pinto and K. R. Branco, "Avens-a novel flying ad hoc network simulator with automatic code generation for unmanned aircraft system," 2017.
- [33] T. Dietrich, K. Silvia and Z. Armin, "A discrete event simulation and evaluation framework for multi UAV system maintenance processes," *2017 IEEE international systems engineering symposium (ISSE)*, pp. 1-6, 2017.
- [34] M. Mozaffari, W. Saad, M. Bennis and M. Debbah, "Drone Small Cells in the Clouds: Design, Deployment and Performance Analysis," *IEEE Global Communications Conference*, pp. 1-6, 2015.
- [35] M. Mozaffari, W. Saad, M. Bennis and M. Debbah, "Efficient Deployment of Multiple Unmanned Aerial Vehicles for Optimal Wireless Coverage," *IEEE Communications Letters*, pp. 1647-1650, 2016.

- [36] M. Mozaffari, W. Saad, M. Bennis and M. Debbah, "Optimal transport theory for power-efficient deployment of unmanned aerial vehicles," *IEEE international conference on communications*, pp. 1-6, 2016.
- [37] M. Mozaffari, W. Saad, M. Bennis and Debbah, "Unmanned aerial vehicle with underlaid device-to-device communications: Performance and tradeoffs," *IEEE Transactions on Wireless Communications*, pp. 3949-3963, 2016.
- [38] D. Pliatsios, P. Sarigiannidis, S. K. Goudos and K. Psannis, "3D Placement of Drone-Mounted Remote Radio Head for Minimum Transmission Power Under Connectivity Constraints," *IEEE Access*, 2020.
- [39] S. Ahmed, M. Z. Chowdhury and Y. M. Jang, "Energy-Efficient UAV Relaying Communications to Serve Ground Nodes," *IEEE Communications Letters*, 2020.
- [40] L. Di Puglia Pugliese, F. Guerriero, D. Zorbas and T. Razafindralambo, "Modelling the mobile target covering problem using flying drones," *Optimization Letters*, 2016.
- [41] D. Zorbas, L. D. P. Pugliese, T. Razafindralambo and F. Guerriero, "Optimal drone placement and cost-efficient target coverage," *Journal of Network and Computer Applications*, 2016.
- [42] V. Sharma, K. Srinivasan, H.-C. Chao, K.-L. Hua and W.-H. Cheng, "Intelligent deployment of UAVs in 5G heterogeneous communication environment for improved coverage," *Journal of Network and Computer Applications*, 2017.
- [43] L. Ruan, J. Wang, J. chen, Y. Xu, Y. Yang, H. Jiang and Y. Zhang, "Energy-efficient multi-UAV coverage deployment in UAV networks: A game-theoretic framework," *China Communications*, 2018.
- [44] Y. Dong, J. Cheng, M. J. Hossain and V. C. M. Leung, "Extracting the Most Weighted Throughput in UAV Empowered Wireless Systems With Nonlinear Energy Harvester," *29th Biennial Symposium on Communications (BSC)*, 2018.

- [45] L. Yang, J. Chen, M. O. Hasna and H.-C. Yang, "Outage Performance of UAV-Assisted Relaying Systems With RF Energy Harvesting," *IEEE Communications Letters*, 2018.
- [46] B. Lee, P. Park, k. Kim and S. Kwon, "The flight test and power simulations of an UAV powered by solar cells, a fuel cell and batteries," *Journal of Mechanical Science and Technology*, 2014.
- [47] G. Mohamed and Z. Sayem, "Analysis of a hydrogen fuel cell-PV power system for small UAV," *International Journal of Hydrogen Energy*, 2016.
- [48] F. Lin, H. Li and X. Zhang, "Research and development of energy monitoring system for solar powered UAV," in *International Conference on Signal Processing (ICSP)*, 2014.
- [49] Y. Sun, D. Xu, D. W. K. Ng, L. Dai and R. Schober, "Optimal 3D-Trajectory Design and Resource Allocation for Solar-Powered UAV Communication Systems," *IEEE Transactions on Communications*, 2019.
- [50] Z. Liu, R. Sengupta and A. Kurzhanskiy, "A power consumption model for multi-rotor small unmanned aircraft systems," 2017.
- [51] B. Acun, B. Lee, F. Kazhamiaka, K. Maeng, M. Chakkaravarthy, U. Gupta, D. Brooks and C.-J. Wu, "Carbon Explorer: A Holistic Framework for Designing Carbon Aware Datacenters," *history*, vol. 1, pp. 2-500, 2020.
- [52] "<https://www.epsilon.com/blog20122017/>," [Online].
- [53] F. Kazhamiaka, C. Rosenberg and S. Keshav, "Tractable lithium-ion storage models for optimizing energy systems," *Energy Informatics*, 2019.
- [54] P. Wiesner, D. Scheinert, T. Wittkopp, L. Thamsen and O. Kao, "Cucumber: Renewable-Aware admission control for delay-tolerant cloud and edge workloads," *arXiv preprint arXiv*, 2022.

- [55] P. Wiesner, D. Scheinert, T. Wittkopp, L. Thamsen and O. Kao, Cucumber: Renewable-Aware Admission Control for Delay-Tolerant Cloud and Edge Workloads, arXiv preprint arXiv:2205.02895, 2022.
- [56] L. Linguet, Y. Pousset and C. Olivier, "Identifying statistical properties of solar radiation models by using information criteria," *Elsevier*, 2016.
- [57] X. You, "Towards 6G wireless communication networks: vision, enabling technologies, and new paradigm shifts," *Science China Information Sciences*, Vols. 64, no. 1, Nov. 2020.
- [58] Z. Xiao, L. Zhu and X.-G. Xia, "UAV communications with millimeter-wave beamforming: Potentials, scenarios, and challenges," [Online].
- [59] J. L. Marins, T. M. Cabreira, K. S. Kappel and P. R. Ferreira, "A Closed-Form Energy Model for Multi-rotors Based on the Dynamic of the Movement," *Brazilian Symposium on Computing Systems Engineering (SBESC)*, 2018.
- [60] S. R. Hassan, N. Shabbir, A. Unbreen, A. U. Rehman and A. Iqbal, "Non Orthogonal Multiple Access: Basic Concepts and Misconceptions," *NFC IEFER Journal of Engineering and Scientific Research*.